TOWARDS DEFINING THE EIF4E INTERACTOME

Aouod Quang Agenor

Department of Biochemistry,

McGill University, Montreal

April 2012

A thesis submitted to McGill University in partial fulfillment of the requirements

of the degree of Master of Science, Biochemistry

ABSTRACT

This work explores the possibility of isolating mRNAs that are bound to eIF4E by photochemical Cross-linking and Immunoprecipitation (CLIP). *In vitro* experiments established that eIF4E cross-linking to mRNA is specific for its cap binding domain and that this complex can be purified by immunoprecipitation. Improved specificity during immunoprecipitation, assessed by protein radiolabeling, was attained by adding a FLAG epitope tag to the amino terminus of eIF4E. As well, an eIF4E mutant, eIF4E (G139D), which was unable to bind to eIF4G yet retained its cap-binding properties was characterized. This works highlights possible future concerns and directions for improving CLIP with the aim of increasing the stringency and quality of immunoprecipitations. Once established, 4E-CLIP could prove to be a powerful tool to screen for novel eIF4E inhibitors and define the eIF4E interactome.

RÉSUMÉ

Cette thèse explore la possibilité d'isoler, par immunoprécipitation, l'ARN lié par un lien covalent à eIF4E par la photochimie. Des expériences *in vitro* établissent que le lien formé entre eIF4E et l'ARNm lors du traitement à UV est spécifique pour son domaine responsable pour interagir avec la coiffe (cap) de l'ARNm et que ces complexes d'eIF4E-ARNm peuvent être immunoprécipités. En ajoutant l'épitope FLAG à l'extrémité N de eIF4E, on a pu améliorer la spécificité des immunoprécipitations, ce qui a été déduit par l'immunoprécipitation de lysats radioactive (S^{35}). De plus, un mutant de eIF4E, G139D, a été caractérisé. Celui-ci a perdu son habileté à interagir avec eIF4G mais retient sa capacité à interagir avec la coiffe d'ARNm. Ce travail amène de l'avant des directions différentes à explorer pour améliorer la qualité des résultats du CLIP. Une fois établi, 4E-CLIP sera un outil indispensable pour trouver de nouvel inhibiteur d'eIF4E et pour définir l'interactome d'eIF4E.

ACKNOWLEDGEMENT

I would like to foremost give my sincerest gratitude and thanks to Dr. Jerry Pelletier, my mentor and research supervisor. I am grateful that he gave me the opportunity to be part of his lab, to work on exciting projects and for his guidance throughout my graduate studies. I would also like to thank him for his support, advice and suggestions for the different projects I've had the chance to undertake.

I would also like to thank Francois Bélanger for his guidance, training and the help he has provided. I would also like to thank the following for their advice, guidance, reagents provided, technical assistance and their friendship: Francis Robert, Regina Cencic, Patrick Sénéchal, John Mills, Abba Malina, Teresa Lee, Gabriela Galicia-Vazquez, Zeina Nasr, Unkyung Shin, Amina Kreps, Sophia Moraitis, Isabelle Harvey, Marylin Carrier.

I am also grateful for the support of my graduate studies by the CIHR Strategic Training Initiative in Chemical Biology (2010) and the FRSQ Master training Award (2011-2012).

TABLE OF CONTENTS

List of Figures

LIST OF ABBREVIATIONS

4E	eIF4E
4E-BP1	eIF4E binding protein 1
4G	eIF4G
Ab	Antibody
Amp	Ampicillin
BSA	Bovine serum albumin
CLIP	Crosslinking and immunoprecipitation
DMEM	Dulbecco's Modified Eagle's Medium
DNA	Deoxyribonucleic acid
DTT	Dithiolthreitol
ECL	Enhanced chemiluminescence
EDTA	Ethylenediaminetetraacetic acid
eIF	Eukaryotic initiation factor
eIF4A	Eukaryotic initiation factor 4A
eIF4B	Eukaryotic initiation factor 4B
eIF4E	Eukaryotic initiation factor 4E
eIF4G	Eukaryotic initiation factor 4G
FBS	Fetal bovine serum

FF	Firefly Luciferase
G139D	eIF4E (G139D) mutant
GDP	Guanosine diphosphate
GST	Glutathione S-transferase
GTP	Guanosine triphosphate
HITS-CLIP	High-throughput CLIP
IgG	Immunoglobulin G
IP	Immunoprecipitation
IRES	Internal ribosome entry site
kDa	Kilodalton
m^7GDP	7-methyl guanosine diphosphate
m^7GpppN	7-methyl guanosine cap structure
m^7GTP	7-methyl guanosine triphosphate
Mnk	MAP kinase signaling integration kinase
mRNA	messenger RNA
MSCV	Murine stem cell virus retroviral expression system
mTOR	Mammalian target of rapamycin
MW	Molecular weight
PAR-CLIP	Photoactivatable-ribonucleoside-enhanced crosslinking and immunoprecipitation
PBS	Phosphate buffered saline

PI3K	Phosphatidylinositol 3-kinases
PK	Proteinase K
PMSF	Phenylmethylsulphonylfluoride
Pre-mRNA	Precursor mRNA
PVDF	Polyvinylidene fluoride
RNA	Ribonucleic acid
RBP	RNA binding protein
Ren	Renilla luciferase
Rheb	Ras homolog enriched in brain
RIP	RNA immunoprecipitation
RPM	Revolution per minute
Supt	Supernatant
SDS-PAGE	Sodium-docecyl sulphate polyacrylamide gel electrophoresis
TSC1/TSC2	Tuberous sclerosis protein 1/Tuberous sclerosis protein 2
tRNA	Transfer RNA
UTR	Untranslated Region
V69G	eIF4E (V69G) mutant
W56A	eIF4E (W56A) mutant

CHAPTER 1: INTRODUCTION

1.1 Overview of mRNA structure

Using genomic DNA as a template, pre-mRNAs are synthesized by RNA polymerase II in the nucleus of eukaryotic cells. They are then processed and exported to the cytoplasm to be translated by the protein synthesis machinery. mRNAs have several distinguishing features which include the cap structure, a 5' untranslated region (5'UTR), a coding region, the 3'UTR and the poly(A) tail[1]. The cap structure is added co-transcriptionally and promotes ribosome recruitment by binding initiation factors during mRNA translation initiation. The 5'UTRs vary in length, degree of secondary structure, occurrence of protein binding sites and/or upstream open reading frames - all of which can influence the efficiency of mRNA translation.

The coding region contains the information that determines the composition and sequence of the amino acids in the polypeptides formed during protein synthesis. The 3'UTR also has elements that can influence translation efficiency. The poly(A) tail promotes recycling of the translation machinery and re-initiation[2]. The amount of proteins synthesized by cells mainly depends on how efficiently these mRNAs are translated. Although all regions of the mRNAs can influence how efficiently they are translated[3], this work focuses on the cap structure and its binding to eIF4E.

1.2 m^7GpppN Cap structure

The cap structure is present in all known eukaryotic cytoplasmic mRNA at the 5' terminus. It is formed by an N7-methylguanosine moiety bound to a nucleotide by a 5'-5' triphosphate bridge (m^7GpppN)[4]. The capping enzyme and RNA (guanine-7-) methyl transferase (RNMT) are found in the nucleus of eukaryotic cells and are responsible for capping newly transcribed mRNA. The capping enzyme creates the 5'-5' triphosphate bridge while RNMT methylates the guanosine at N7, producing a cap 0 structure (Figure 1). In yeast, mRNAs have no other modifications but in higher eukaryotes, the mRNA is further methylated at the 2'O-ribose of the first and/or second transcribed nucleotides, producing cap 1 and cap 2, respectively[5]. Although the enzyme responsible for producing the cap 2 structure has yet to be identified in mammals, hMTr1 was recently identified and characterized and found to catalyze 2'-*O*-methylation of cap 1[6]. The function of these secondary methylations has yet to be elucidated. *In vivo* knockdown of hMTr1 had no obvious effects on overall cellular viability despite initial *in vitro* experiments demonstrating a moderate increase in translation efficiency[7]. Also, if the first nucleotide is an adenosine residue, further methylation of the 2'-*O*-dimethyladenosine is possible at the *N6* position of the adenine[8].

The cap structure plays important roles in various processes of mRNA biogenesis and function. It imbues a protective effect against mRNA degradation by 5'–3' exonucleases and plays a role in pre-mRNA processing[9]. The CBP20 subunit of the CBP20/80 complex binds to the cap structure in the nucleus and promotes splicing by enhancing the interaction between U1 snRNP and the 5'

splice site of pre-mRNA. CBP20/80 also promotes nucleocytoplasmic transport of the pre-mRNA[10]. This said, the most studied aspect of the cap structure is its interaction with eIF4E, which is a critical step for cap-dependent mRNA translation.

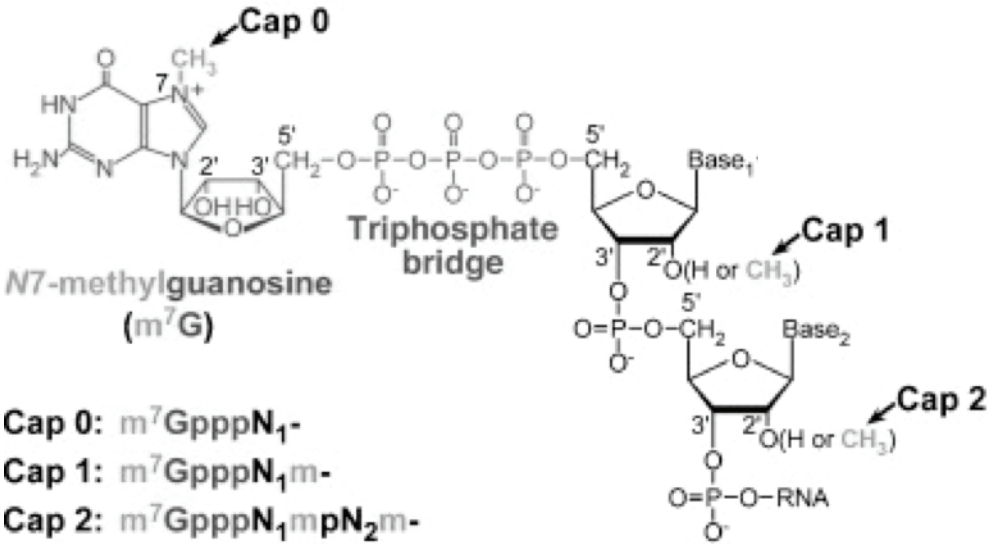

Figure 1: Eukaryotic Cap structure.

The cap structure is located at the 5' terminus of eukaryotic mRNAs. It is composed of an N7-methylguanosine moiety linked to the first nucleotide by an inverted 5-5' triphosphate bridge. In higher eukaryotes, the 2'O ribose of the first 2 nucleotides is also methylated to form the cap 2 structure. (Adapted from Ogino *et al.*, 2011)[5].

1.3 eIF4E binds mRNA cap structure and its affinity is modulated by the 5'UTR region

eIF4E is a 25 kDa protein that recognizes and binds the m^7GpppN cap structure of the mRNA, promoting initiation of cap-dependent mRNA translation. The structure of eIF4E bound to m^7GDP has been determined by X-ray crystallography[11] and NMR[12]. When bound to m^7GDP, eIF4E resembles a cupped hand. It is composed of an eight-stranded antiparallel curved β-sheet, backed on its convex surface by three long α-helices. m^7GDP is bound to eIF4E in a narrow pocket on the concave surface of eIF4E. This interaction occurs mainly by π-π stacking between the side chains of 2 conserved tryptophans (amino acids 56 and 102) of eIF4E and the positively charged 7-methylguanine of the cap[13]. There is also formation of 3 hydrogen bonds and a Van der Waals interaction between the cap N7-methyl group and a conserved tryptophan (107). Mutation of these tryptophans residue abolishes eIF4E cap binding affinity[14,15].

When bound to eIF4G, which also interacts strongly with mRNA, eIF4E's affinity for the cap structure is tenfold higher[16]. However, secondary structure in the 5'UTR of mRNA can modulate the efficiency of binding of the eIF4F complex (formed by eIF4E, eIF4G and eIF4A). Short 5'UTRs (20-50 nucleotides) with minimal secondary structure interact efficiently with eIF4F while more structured 5'UTRs show less favorable interaction with eIF4F[17]. Not only can the thermodynamic stability of these secondary structures inhibit translation efficiency, but the position of these structures is also an important factor that can

cause inhibition. Translation is less efficient when moderate secondary structure is situated close to the cap structure compared to if it is further downstream of the cap[18], presumably due to hindrance of the interaction of eIF4G with mRNA and eIF4E with the cap structure[19].

1.4 Overview of protein synthesis.

Protein synthesis or mRNA translation is a fundamental mechanism. This process can be separated into 3 main steps: initiation, elongation and termination. After recruitment to the mRNA and correct positioning at the initiation codon, the ribosome, a large RNA-protein complex, synthesizes a polypeptide N-terminus to C-terminus by tracking along the coding region of the mRNA and catalyzing the formation of amide bonds between amino acids. The sequence of triplets of nucleotides (codons) is used as a blueprint and dictates which amino acid is incorporated into the nascent polypeptide. Selectivity of amino acid addition is made possible through complementary base pairing of the mRNA's codon with a specific transfer RNA (tRNA) which is recruited into the ribosome. The amino acid bound to the tRNA is delivered to the ribosome and added to the elongating peptide chain. Once the ribosome reaches the stop codon, the peptide is released and the translation machinery dissociates from the mRNA. Initiation is the most highly regulated step of protein synthesis[20].

1.5 Initiation of cap-dependent mRNA translation.

The rate-limiting step in eukaryotic cap dependent translation initiation is the binding of eIF4F to the cap structure (Figure 2). eIF4F is composed of the scaffold protein, eIF4G; the cap binding protein, eIF4E; and the DEAD-box RNA

helicase, eIF4A. Once eIF4F binds to the cap structure, it is thought that the RNA binding proteins, eIF4B and eIF4H, interact with eIF4A to promote RNA unwinding[21,22]. This facilitates binding of the 40S ribosome to the mRNA 5'UTR. The 40S ribosome associates with eIF1, eIF1A, the Met-tRNA$_i^{Met}$ •GTP•eIF2 complex, eIF3 and eIF5A to form a 43S pre-initiation complex. Interaction between eIF3 and eIF4G allows recruitment of the small 43S ribosomal unit to the mRNA.

Following ATP hydrolysis, the 40S ribosome and associated factors are thought to scan the 5' untranslated region (5'UTR) of the mRNA in a 5' to 3' direction until it reaches the AUG initiation codon. The consensus sequence for optimal initiation is GCC(A/G)CCAUGG[20]. Whether ATP hydrolysis is required for scanning or just ribosome loading has yet to be elucidated. eIF1 allows the ribosome to differentiate between AUG and non-AUG codons and therefore recognize the start codon. Once positioned at the start site, GTP hydrolysis of eIF2-GTP by the eIF5A subunit, a ribosome dependent GTPase, stimulates the release of eIF2-GDP. This is followed by correct base pairing between the initiation codon and the anticodon of the Met-tRNA$_i^{Met}$. The initiation factors are released from the complex and eIF5B is recruited. Another round of GTP hydrolysis causes the 60S to be recruited, forming the 80S complex and setting the stage for the elongation phase of protein synthesis[23].

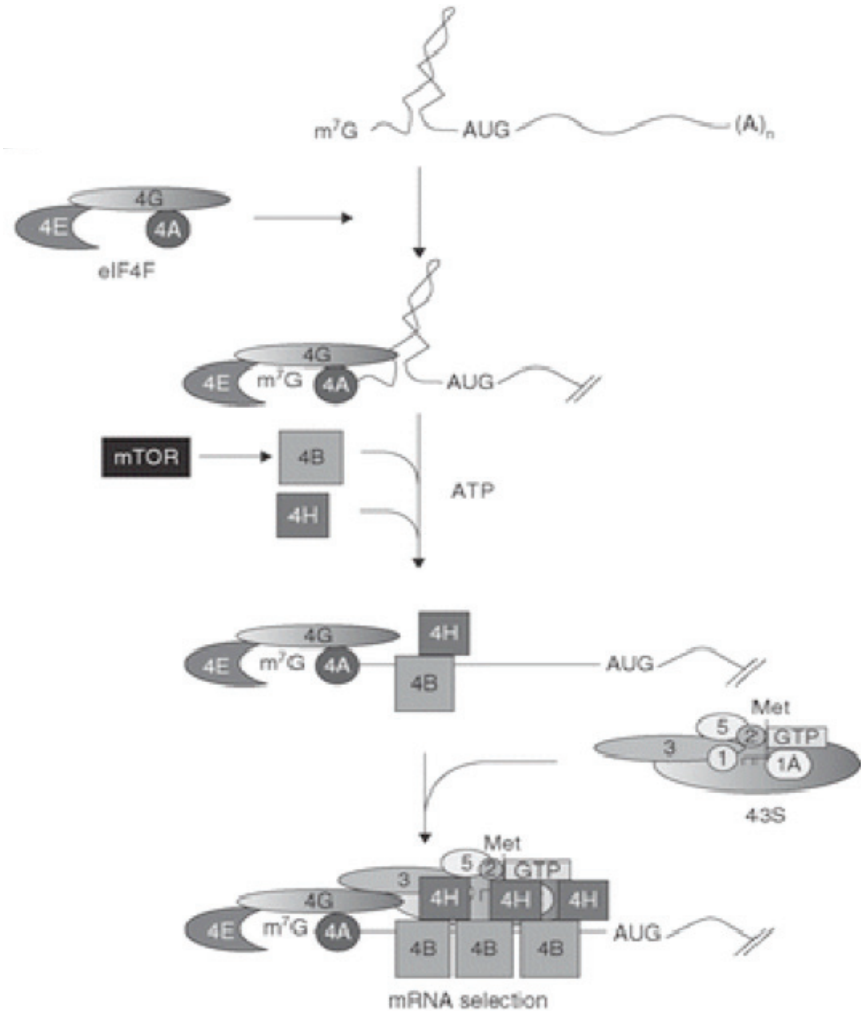

Figure 2: Schematic Diagram of Translation Initiation.

eIF4F (composed of eIF4A, eIF4E and eIF4G) binds the mRNA by recognition of the 5' cap structure via eIF4E. eIF4B and eIF4H are recruited and stimulate eIF4A unwinding of the mRNA 5'UTR secondary structure. The 40S ribosome and associated factors are then recruited to the mRNA template and in an ATP-dependent process scan the mRNA for the initiation codon, AUG (Adapted from Robert *et al*. 2009)[24].

1.6 eIF4E availability is the main regulator of translation initiation.

Protein synthesis, being a fairly energetically costly process, is mainly regulated at the initiation step. Being the least abundant initiation factor[24], eIF4E availability for the eIF4F complex is the main regulator of initiation. Formation of the eIF4F complex can be impeded by sequestration of eIF4E by the eIF4E-binding proteins (4E-BPs). When unphosphorylated, the 4E-BPs bind eIF4E through a common binding site shared with eIF4G; eIF4E binding to the 4E-BPs and eIF4G is therefore mutually exclusive[25] (Figure 3). There are 3 related homologs of the 4E-BPs in mammals of which 4E-BP1 is the best characterized. The 4E-BPs and eIF4G all share a conserved Tyr-X-X-X-X-Leu-ϕ 4E-binding consensus motif[26] (where X is a any amino acid and ϕ is a hydrophobic amino acid). Hyperphosphorylation of 4E-BP reduces its affinity for eIF4E, allowing eIF4E to interact with eIF4G, thus stimulating eIF4F formation and increasing mRNA translation initiation rates[27]. Phosphorylation of 4E-BP1 is sequential: Thr37, Thr46, Thr70 and then Ser65[28]. Stimulation of 4E-BP phosphorylation is dependent on growth signals and cellular energy levels, through the mTOR (Mammalian Target of Rapamycin) pathway[29].

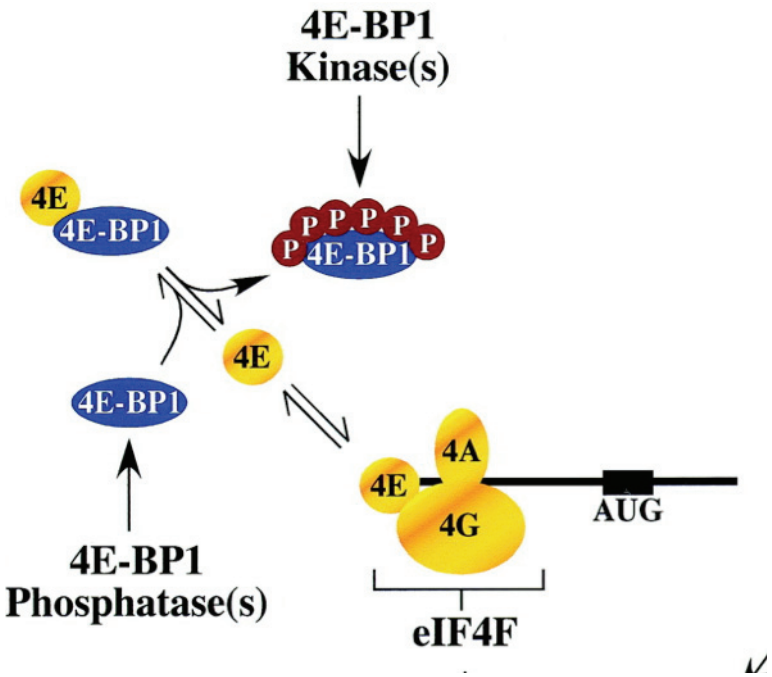

Figure 3: eIF4G and 4E-BP1 binding to eIF4E is mutually exclusive.

eIF4E activity is regulated by shuttling between the active eIF4F complex and the inhibitory complex 4E-BP/eIF4E. Phosphorylation of 4E-BP1 dampens its affinity with eIF4E, resulting in stimulation of mRNA translation. (Adapted from Shah *et al*. 2009)[29].

1.7 mTOR is an upstream regulator of cap-dependent translation

The mTOR (mammalian target of rapamycin) pathway is a key regulator of translation initiation and its regulation is usurped in many human tumors. mTOR integrates signals from amino acid imbalances, mitogens, growth factors and hormones, as well as nutrient and energy availability, to regulate translation initiation (Figure 4) amongst other effects. Extracellular signals can activate phosphatidylinositol 3-kinase (PI3K), a signal transducer. This leads to the phosphorylation of phospholipid phosphatidyl inositol-4,5-bisphosphate (PIP2) at the plasma membrane to generate phosphatidyl inositol-3,4,5-triphosphate (PIP3). Inactive AKT, a serine/threonine-specific protein kinase, and 3-phosphoinositide-dependent protein kinase 1 (PDK1) are then recruited to the plasma membrane through their PH domains, which recognize PIP3. PDK1 then phosphorylates and activates Akt. By phosphorylating tuberous sclerosis protein 2 (TSC2), Akt in turn destabilizes a complex formed by Tuberous sclerosis protein 1 and Tuberous sclerosis protein 2 (TSC1/TSC2), which normally inhibits the GTPase, Rheb (ras homolog enriched in brain)[30].

TSC1/TSC2 promotes Rheb GTPase function, keeping it in its inactive Rheb-GDP state. Disruption of TSC1/TSC2 leads to an increased levels of active Rheb-GTP, which in turn activates the mTORC1 complex. This complex is composed of mTOR and two positive regulators of its function (raptor and LST8). Active mTORC1 phosphorylates downstream targets such as the 4E-BPs,

reducing their affinity for eIF4E. eIF4E then becomes available to assemble into the eIF4F complex and protein synthesis initiation is stimulated[31].

mTOR can also stimulate translation initiation in a 4E-BP independent manner. Activated mTOR/raptor complex can phosphorylate S6 kinase 1 (S6K1) bound to eIF3, which mediates its dissociation and allows it to interact with PDK1. PDK1 activates S6K1 by phosphorylating S6K1 at residue Thr 229[32]. This phosphorylation activates S6K1, which can now phosphorylate and activate eIF4B. S6K1 can also mediate the stability of PDCD4, a tumor suppressor that sequesters eIF4A and inhibits formation of the eIF4F complex by targeting it for ubiquitination and degradation[33]**.** The interaction of mTOR with eIF3 also augments the association between eIF3 and eIF4G[34]. The mTOR pathway is inhibited by rapamycin, which leads to lowered protein synthesis.

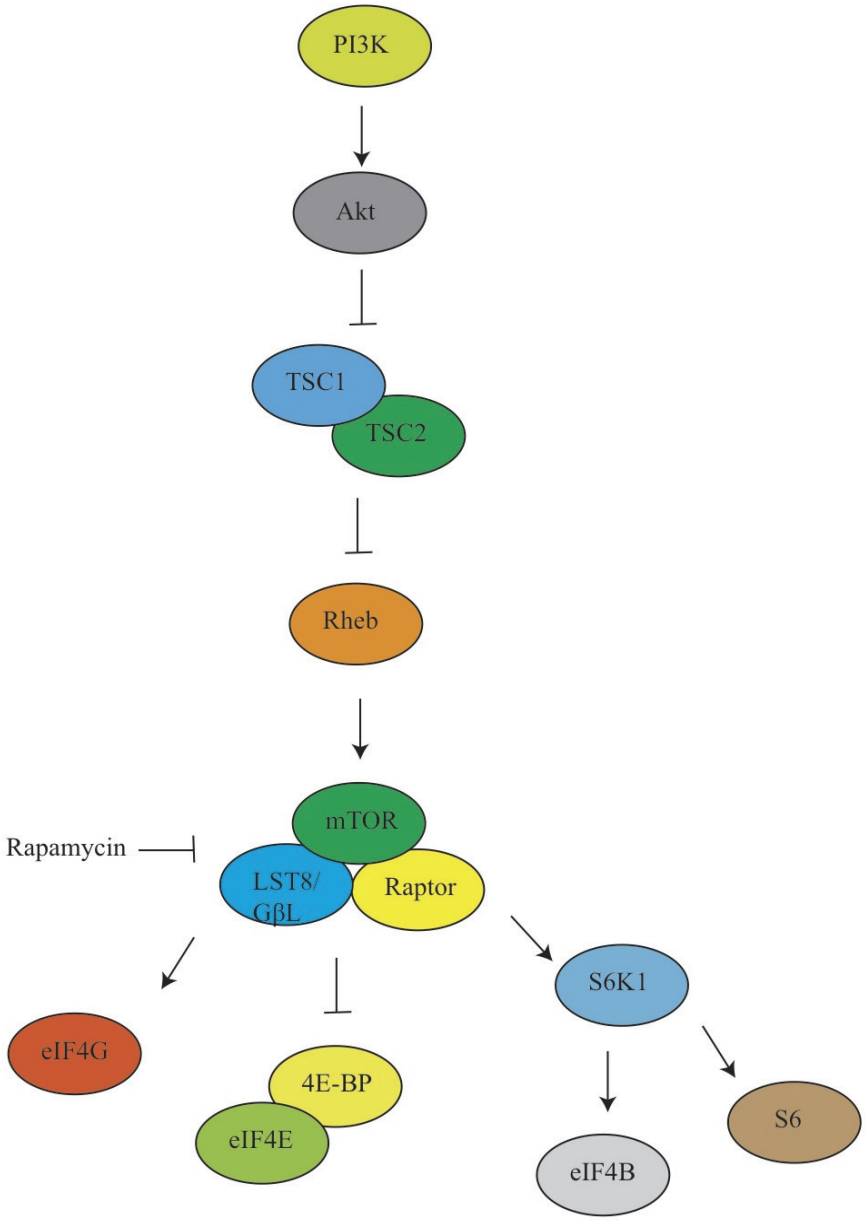
PI3K
Akt
TSC1
TSC2
Rheb
mTOR
Rapamycin
LST8/
GβL
Raptor
S6K1
eIF4G
4E-BP
eIF4E
eIF4B
S6

Figure 4: The mTOR pathway regulates protein synthesis.

Extracellular signals activate PI3K, which leads to activation of Akt. Akt destabilizes the TSC1/TSC2 complex, which normally inhibits Rheb. Activated Rheb activates the mTOR/raptor/LST8 complex (mTORC1), which causes phosphorylation of downstream targets and dramatic increase in eukaryotic translation initiation.

1.8 Deregulated eIF4E levels drive oncogenesis

Cancer cells, which are characterized as having uncontrolled growth, would greatly benefit from increased protein synthesis. It is therefore no surprise that many translation initiation[35] and elongation[36] factors are associated with oncogenesis. Here, we will focus on eIF4E's role in tumorigenesis. A wealth of experiments have shown that overexpression of eIF4E can drive oncogenesis[37]. Its overexpression has been associated with transformation in fibroblasts[38], acceleration of tumor onset and chemoresistance[39]. Antisense oligonucleotides targeting eIF4E significantly curtail oncogenic transformation[40]. Correspondingly, expression of constitutively active 4E-BP (T37 and T46 or F114 sites mutated to alanine), which binds eIF4E and inhibits eIF4F formation, reduces cell size[41], inhibits G1 cell cycle progression, blocks c-myc induced transformation[42] and prevents tumor growth[43]. In clinical settings, high levels of eIF4E are linked to later tumor stages, more aggressive tumors and poorer outcome[44]. Moreover, phosphorylation of eIF4E on S209 by Mnk1/2, a downstream effector of Mitogen-activated protein kinases, has been shown to promote eIF4E's transformation potential[48]. Although the reason for this is not totally understood, it may stabilize the interaction of eIF4E within the eIF4F complex[45] or may reduce eIF4E's affinity to the cap structure[46].

Given eIF4E's role in cap dependent translation, one might assume that its oncogenic potential is mainly due to increased global protein synthesis because of higher expression of eIF4E. Yet overexpression of eIF4E only mildly increases

protein synthesis[47]. In fact, a modest increase of only 2 to 3 fold in expression of eIF4E is sufficient to elicit oncogenesis[48] without greatly affecting global protein synthesis. Also, although the cap structure is crucial for efficient translation *in vitro*, surprisingly, knockdown of the cap binding protein, eIF4E, in cell cultures only modestly decreases translation[49] in cells. Some hypotheses have been brought up to explain this discrepancy. One of them is that there might be some regulatory mechanism present in cells that no longer functions in extracts. A more favored explanation is that some mRNAs are very efficiently translated and eIF4E knockdown does not significantly affect them. Nevertheless, this suggests that although a lot is known about cap dependent translation *in vitro,* our knowledge of eIF4E's roles *in vivo* remains rudimentary.

Selective and disproportionate upregulation of the translation of specific mRNAs[50] is the accepted model explaining eIF4E's oncogenic potential. While modulation of eIF4E levels does not dramatically alter global protein synthesis, the expression levels of a subset of mRNAs are greatly affected. Given the important role of secondary structure in the 5' UTR of mRNA for modulating eIF4F binding (see section 1.3), it is believed that mRNAs with highly structured 5'UTRs rich in GC content (weak mRNA), are usually inefficiently translated due to their low affinity for eIF4E/eIF4G[51] although determination of transcription-wide direct interaction of eIF4E with mRNA has yet to be elucidated *in vivo* in a robust manner. The current model proposes that these weak mRNAs are outcompeted by abundant and more efficiently translated transcripts (strong mRNA) in cells with normal levels of free eIF4E. When eIF4E is overexpressed,

cap dependent translation initiation is less selective. Transcripts which are usually translated at lower levels due to inefficient eIF4F binding are no longer outcompeted by more efficiently transcribed strong mRNAs.

Many findings have supported this model. Many mRNAs linked to cancer have highly structured 5'UTRs and are usually very inefficiently translated because of inefficient interaction with eIF4F (see section 1.3). In fact, eIF4E can specifically modulate the expression of many proto-oncogenes, anti-apoptotic proteins and growth factors associated with cancer such as c-Myc, cyclin D1, Mcl-1, survivin, VEGF, FGF2, MMP3, MMP9[52]. Furthermore, inhibition of eIF4F assembly by rapamycin has been shown to reduce the translation of these mRNA[53]. Treatment with this drug inhibits the mTOR pathway and leads to dephosphorylation of 4E-BP1, which can now bind eIF4E and prevent eIF4F formation. Of note, other inhibitors of eIF4F such as the eIF4A inhibitor, silvestrol, have been shown to preferentially reduce translation of weak mRNAs[54]. Another example of this model is the positive feed forward loop between eIF4F and c-Myc[55]: the c-Myc transcript contains relatively stable secondary structures in its 5'UTR. c-Myc promotes translation initiation by upregulating transcription of eIF4AI, eIF4E and eIF4GI subunits mRNA[56]. The increased abundance of initiation factors in turn promotes efficient translation of c-Myc mRNA. Despite the current knowledge, our understanding of specific regulation of mRNAs by eIF4E remains incomplete.

None of the data implicating eIF4E as a driver of oncogensis directly evaluates the interaction of eIF4E with mRNAs in cells. This is also an

impediment to the development of drugs targeting eIF4E-mRNA interaction, since direct measurement of this process in cells or animal models has not been possible so far. One strategy to directly evaluate eIF4E binding *in vivo* would be by photochemical cross-linking of eIF4E to mRNA and immunoprecipitating the eIF4E-mRNA complexes followed by identification of the associated transcripts.

1.9 RNA binding proteins and their RNA targets

Advances made to determine which transcripts RNA binding proteins (RBP) interact with has not kept up with those made in studies of DNA binding proteins. Early attempts to identify RBP targets *in vitro* were hindered by poor ability to discover consensus sequences, the determination of only very short binding sites[57] and poor prediction of novel RNA targets in cells[58]. This is not surprising given that *in vitro* experiments usually fail to reproduce the complex environment governing the transient interactions of molecules in cells. Some initial attempts to co-immunoprecipitate RBP with their RNA targets (RNA immunoprecipitation (RIP)) have shown modest success but were always plagued by a low signal to noise ratio. The high amount of non-specific pulldown is attributable to technical obstacles, such as the inability to wash stringently or the co-immunoprecipitation of other RBPs, and the fact that RNA, given its dynamic nature, tends to transiently bind to RBPs. In fact, it has been observed that RBPs can artificially re-associate with RNA during the process of co-immunoprecipitation[59] and that the conditions of RIP could selectively abolish some RBP-RNA interactions while preserving others with the same RBP intact[60],

putting into question the physiological relevance of RNA targets identified in some studies.

The requirement for stringent experimental conditions to obtain the best signal to noise ratio, yet being mild enough to preserve protein-RNA interactions, was an ever present major issue in RIP. For example, a majority of RNA targets found to bind fragile-X-mental retardation protein (FMRP) by RIP failed to validate as direct binding partners, despite the many precautions included in the experimental design such as the elimination of sequences isolated by RIP from a FMRP null mouse, selection for enriched RNA compared to total transcript representation in cells and bioinformatics-based screening of the RIP results. The high number of false positive was mainly caused by unavoidable co-immunoprecipitating RBPs in complex with FMRP during RIP[61]. Better methods to identify RBP targets were needed.

1.10 Photochemical cross-linking

A solution to some of the problems associated with RIP is to crosslink the protein to RNA *in vivo* before cell lysis. This can be achieved by photochemical cross-linking. UV induced cross-linking between protein and RNA was first demonstrated between tRNA and tyrosyl-tRNA synthetase[62] *in vitro* and it was soon realized that this technique could also be applied *in vivo*[63]. The technique though was not used to identify RNA targets by sequencing until recently because it was believed that the UV crosslinking efficiency would be too low to isolate

enough material[64] and since cross-linking had been established as a method to block reverse transcriptase[65] that this would generate templates that could not be converted into cDNA. The latter would prevent analysis of RNA recuperated from IP of crosslinked RNA.

The basic idea behind the technique is that, when RNAs and RBPs are treated with UVB light, covalent bonds are formed between closely interacting nucleotides and amino acids. Although the mechanism is not totally understood, it is believed that the radiation is absorbed by nucleic acid bases and that free radicals are created that chemically react with nearby peptides to form covalent bonds[66]. Pyrimidines are more prone to react and covalently bind to cysteine, lysine, phenylalanine, tryptophan and tyrosine residues at UV_{254}[67]. The formation of these bonds allows for improved stringency during purification of the protein-RNA complexes from cellular extracts. One widely used method of isolating protein-RNA complexes is by immunoprecipitation (cross-linking and immunoprecipitation; CLIP) although other methods are possible such as Ni^{2+} column purification of His-tagged proteins[68].

An advantage of photochemical cross-linking is that the low energy required for the process does not induce formation of covalent bonds between amino acids, conferring RNA-protein specificity. This is in contrast to formaldehyde-based chemical cross-linking which causes protein-protein cross-links in addition to covalent bonds between nucleic acid and proteins. Formaldehyde cross-linking, however, is reversible, unlike photochemical cross-linking. Despite not forming protein-protein cross-links, UVB treatment has been

shown to create covalent bonds between RNAs[69]. Another advantage is that it is also possible to couple the technique with deep-sequencing methods to generate large datasets allowing for better interpretation and modeling of RBPs targets. The biggest advantage of UVB treatment is the possibility of forming covalent bonds between closely interacting RNAs and proteins in intact cells and tissues, thereby generating biologically relevant data. Crosslinking of protein to RNA in cells was indeed first undertaken with hnRNPs where these proteins were covalently bound to polyadenylated RNA by UV irradiation[70] in the 80's. Ever since, the technique has in fact been successfully used in many different settings to identify RBP targets[71,72,73].

1.11 Cross-linking and Immunoprecipitation (CLIP)

CLIP was first used to identify 340 RNA tags which cross-linked to the RNA binding protein, NOVA[74]. Further studies allowed the same laboratory to refine the technique for high throughput sequencing and generate larger datasets enabling the generation of a robustly predictive NOVA splicing regulatory map. It also led to the discovery of a novel role for NOVA in alternative polyadenylation[75]. The technique has subsequently been used to identify targets of many other RBPs including PTB[71], Fox2[72], Khd1[73] and hnRNP A1[76], as well as providing new insight into the mechanism of action of some of the targets [77]. The technique was also used to map protein-RNA binding points by identifying sites at which mutations[78] or reverse transcription blocks occurred[79] presumably caused by residual amino acids still covalently bound to the RNA. CLIP has

undergone further refinements and each of these are associated with a different acronym: PAR-CLIP[80], which uses photoreactive nucleotides analogues to increase cross-linking efficiency, HITS-CLIP[81], which has been optimized for SOLEXA deep-sequencing, iCLIP[82], used to identify protein-mRNA contact points by identifying mutations in the cDNA and CRAC[83], in which His-tagged proteins are isolated by Ni^{2+} column.

1.12 CLIP limitations

Despite the potential of CLIP, there are still some concerns and limitations associated with the technique. The most important is the issue of specificity and stringency, which greatly depends on the quality of the antibody and the biochemical method used to isolate the RNAs. The technique is therefore limited in that it requires antibodies that have very high specificity and that yield low background by avoiding cross-reactivity with other unrelated proteins and enrichment of these proteins during immunoprecipitation. The addition of an epitope tag to the protein of interest to increase stringency as performed with CRAC[84] is one method to circumvent this problem. However ectopic overexpression of RNA binding proteins will always bring up questions of physiological relevance for any subsequently identified RNA motifs.

Another concern is the low efficiency of UV cross-linking. Given the fact that CLIP typically yields 10^5 to 10^6 unique reads[85], this would be a problem only if the number of different RNA targets of the RBP of interest was on the same

order of magnitude in complexity. One might be concerned that UV treatment of cells will activate the RNA/DNA damage repair pathways possibly affecting results. However, these responses usually take 30 min at 37^{o}C to activate[86] and UV treatment is usually performed for less than 10 min and on ice, after which point the cells are immediately lysed. This said, there is the possibility that some sequences are preferentially isolated by this approach creating a potential bias since the mechanism of UV cross-linking is poorly understood. Nevertheless, CLIP remains a powerful method that has a young, but robust record of identifying RNA targets of RBPs and is a valid method to probe for these interactions *in vivo*.

1. 13 eIF4E and CLIP

This work highlights an effort to probe for mRNAs that interact with eIF4E using CLIP. It has been previously shown *in vitro* that eIF4E can be cross-linked to mRNA cap structures when subjected to UV_{254} light[87]. The proposed strategy is to develop and fine-tune CLIP to immunoprecipitate eIF4E cross-linked to mRNA by treatment with UV light, followed by deep-sequencing of the mRNA 5'ends (Figure 5). Developing this technique would make it possible to create assays that directly evaluate binding of eIF4E to the cap structure of mRNAs *in vivo* and in animal models, of which currently no assay exists. As well, one could compare how the representation of eIF4E-interacting mRNAs (and to a degree translation initiation) changes between cells under different physiological

situations or upon treatment with drugs that affect eIF4F activity, such as rapamycin.

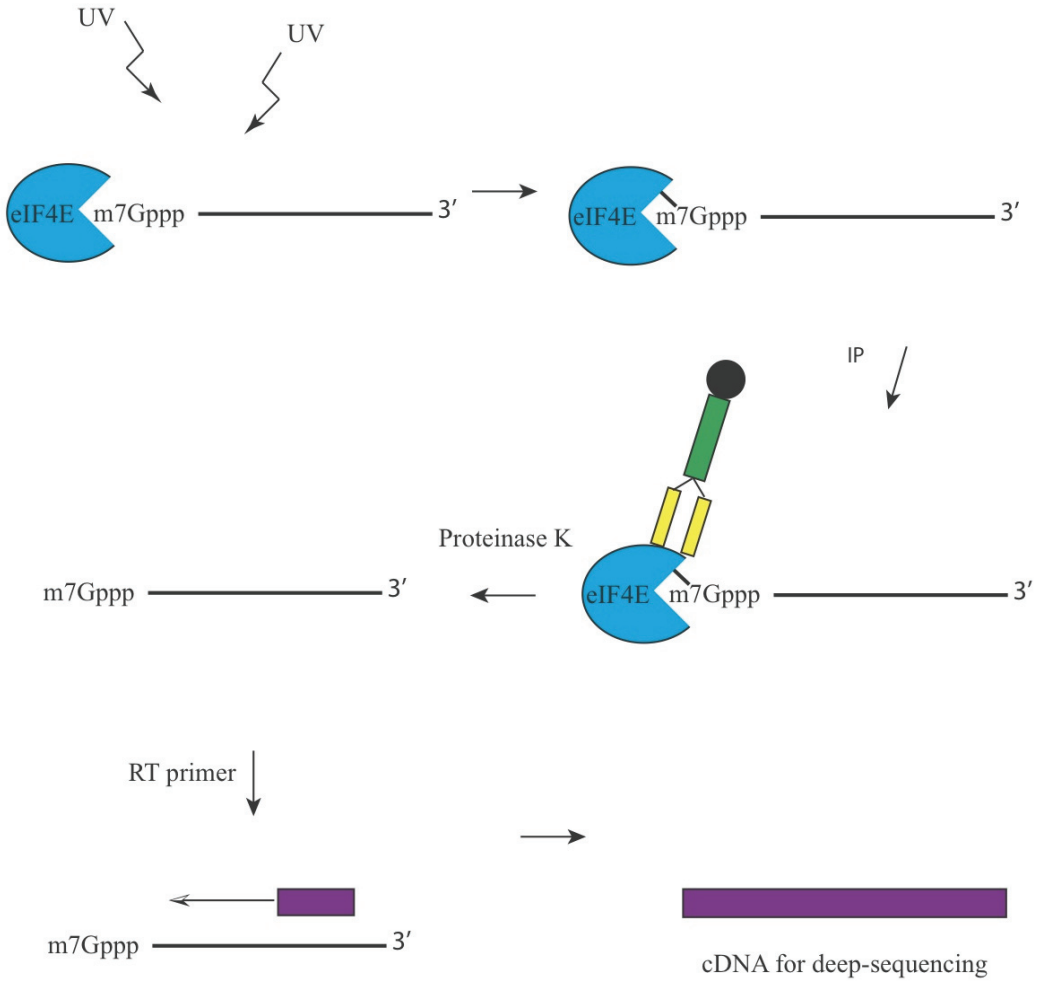
UV
UV
eIF4E
m7Gppp
3′
eIF4E
m7Gppp
3′
IP
Proteinase K
m7Gppp
3′
eIF4E
m7Gppp
3′
RT primer
m7Gppp
3′
cDNA for deep-sequencing

Figure 5: Schematic representation of basic 4E-CLIP

Schematic representation of 4E-CLIP. Cells are irradiated with UV light. RNA bound to eIF4E will crosslink (formation of a covalent bond) and these complexes can be isolated by immunoprecipitation. The samples can be treated with DNase to eliminate any DNA co-purifying non-specifically. The RNA is liberated from the protein by digestion of proteins with Proteinase K, which is subsequently reverse transcribed and sequenced.

CHAPTER 2: MATERIALS AND METHODS

2.1 Mutagenesis and Recombinant DNA techniques

Mutations of the murine eIF4E cDNA [HPL37-39AAA (CACCCTCTA to GCTGCCGCT), V69G (GTT to GCC) and G139D (GGA to GAC)] was performed by overlap PCR[88] using mismatched complementary DNA primers (Biocorp) directed to the target site and cloned into the *Bgl*II site of the MSCV retroviral vector. For HPL37-39AAA, HPL_FW (5'-ACTATATTAAAGCTGCCGCTCAGAACAGGTGGGCACTCTG-3'), and 3'oligo (5'-GGAACAATAGATCTTTAAACAACAAACCTATTTTTAG-3') were used as primers in a PCR containing Platinum Taq HiFi (Invitrogen) following the cycling parameters ([0.5 min 94^{o}C, 1 min 55.0^{o}C, 1.5 min 72^{o}C, 2 min 94^{o}C] X 25 times) using the murine eIF4E cDNA as template. In parallel, a similar PCR was performed with HPL_RV (5'-ACCTGTTCTGAGCGGCAGCTTTAATATAGTGCTCTGGGTT-3') and FLAG-5' (GACTACAAAGACCATGACGGTGATTATAAAGATCATGATATCGATTA CAAGGATGACGATGACAAGCTTATGGCGACTGTGGAACCGG-3') primers in a separate PCR. The products were gel purified using an EZ-10 spin column gel extraction kit (Bio-Basic). One hundred nanograms of both PCR products were then combined and used in an overlap PCR. One cycle (4 min 94^{o}C, 3 min 57.0^{o}C, 13 min72^{o}C, 2 min 94^{o}C) was performed followed by

addition of external oligos (3'oligo and FLAG-5' primers) and the PCR was continued as follows, ([0.5 min 94^{o}C, 1 min 55.0^{o}C, 1.5 min 72^{o}C, 2 min 94^{o}C] X 25 times). Final PCR products were gel purified, digested with *Bgl*II/*BamH*I and cloned in the retroviral vector MSCV (*Bgl*II site). PCRs were performed similarly to introduce the mutations V69G and G139D using the primer pairs:

V69G_FW (5'-GTTTGATACTGGCGAAGACTTTTGGGCTCTATA-3')

V69G_RV(5'-AAAAGTCTTCGCCAGTATCAAACTTAGAGATCA-3')

G139D_FW(5'-GTGCCTTATTGACGAATCTTTCGATGACTACAG-3')

G139D_RV (5'-CGAAAGATTCGTCAATAAGGCACAGCAGTGTCT-3')

FLAG-eIF4E and FLAG-eIF4E(W56A) were cloned using 3'oligo and FLAG-5' as primers and MSCV/eIF4E or MSCV/eIF4E-W56A cDNA as template in a standard PCR ([0.5 min 94^{o}C, 1 min 55.0^{o}C, 1.5 min 72^{o}C, 2 min 94^{o}C] X 25 times). The PCR products for all mutants were also sub-cloned into pET-15b vector (*Nco*I/*BamH*I sites) for bacterial expression. All resulting mutations were verified by sequencing (McGill University and Génome Québec Innovation Centre).

2.2 *In vitro* crosslink of eIF4E with radioactive cap labeled mRNA

RNA synthesis was performed using T7 RNA polymerase (NEB) for 2 hours at 37^{o}C in 40 mM Tris-$HCl_{7.9}$, 6 mM $MgCl_2$, 10 mM dithiothreitol, 2 mM spermidine, 500μM ATP, 500 μM CTP, 500 μM UTP, 500μM GTP and 400

units/mL of RNAse inhibitor (NEB). The RNA was then purified from the reaction mix by phenol/chloroform extraction, followed by chloroform extraction and G50 column purification. RNA was precipitated overnight at -80^{o}C with 1/10 volume of NH_4OAc pH 5.2 and 2.5 volumes of EtOH. Samples were centrifuged at 13 000xg for 10 min at 4^{o}C. The RNA pellet was washed with 70% EtOH, resuspended in RNase-free water and quantified with a NanoDrop spectrophotometer (Thermo Scientific). Transcripts were cap-labeled with vaccinia virus guanylyltransferase in the presence of [α-^{32}P]GTP and S-adenosyl-L-methionine as previously described by Monroy G *et al*[89].

Photochemical cross-linking was essentially performed as described by Ulmanen *et al*[90]. Briefly, 100,000cpm of ^{32}P cap labeled CAT mRNA and purified murine eIF4E were incubated in a total volume of 20 μL in eIF4E binding buffer (25mM $Hepes_{7.5}$, 2mM DTT, 0.2mM spermidine, 0.5mM $Mg(OAc)_2$) at 30^{o}C for 10 min. Samples were then irradiated at 254 nm at 4^{o}C for 15 min at a distance of 4 cm with a UVP Multiple-Ray Lamp (Fisher). Samples were treated with 0.5 mg/mL RNAse A (NEB) at 37^{o}C for 30 min. Cross-linked reactions were diluted in RIPA buffer (25mM Tris-$HCl_{7.6}$, 500mM NaCl, 1% NP-40, 1% Sodium deoxycholate, 0.1% SDS) and immunoprecipitations (see section 2.3) performed with anti-eIF4E antibodies (RN001P (MBL) or A301-153A (Bethyl)). After extensive washing, Laemmli buffer was added and samples were separated on 12% SDS-polyacrylamide gel. The gel was dried and exposed to film (BioMax XAR scientific imaging film (Kodak)) overnight at -80^{o}C. The use of m^7GpppG

or GpppG capped radioactive RNA and the addition of 20 μM m^7GDP to the cross-linking reaction were used to determine cap specificity.

2.3 Immunoprecipitation

Protein A Sepharose (GE healthcare) was prepared for IP by washing twice with PBS and once with $RIPA_{NaCl}$ buffer (25mM Tris-$HCl_{7.6}$, 500mM NaCl, 1% NP-40, 1% sodium deoxycholate, 0.1% SDS). Protein A Sepharose beads were collected by centrifugation at 5000xg for 1 min and resuspended in 3 beads volumes of RIPA to create a 25% Protein A Sepharose slurry. An aliquot of 50 μL of this mix (per IP sample) was transferred to a clean eppendorf tube.

The Protein A Sepharose slurry aliquot was incubated with 1 mL of RIPA buffer and 5μg of anti-eIF4E antibody (RN001P (MBL), A301-153A (Bethyl)) or IgG (MBL) and rotated end-over-end for 1 hour at 4^{o}C. After washing once with PBS, the antibody bound Protein A Sepharose beads were blocked for one hour end-over-end at 4^{o}C with 5% BSA in RIPA buffer. These were then washed once with RIPA and added to the extracts in which the IP of eIF4E was desired. The volume was adjusted to 1mL with RIPA and samples were incubated end-over-end for 3 hours at 4^{o}C. Samples were then washed 3X with $RIPA_{NaCl}$ buffer. Small aliquots of the supernatant and IP were collected, fractionated on an SDS-polyacrylamide gel and probed by Western Blot using anti-eIF4E (BD sciences) and/or M2 anti-FLAG (Sigma-Aldrich) antibodies. HRP conjugated secondary antibodies were from Jackson Immuno Research.

A similar protocol was performed for anti-FLAG immunoprecipitations with the following modifications. Protein G Sepharose (GE healthcare) and M2 (anti-FLAG (Sigma) were used for IP. Flag lysis buffer (50mM Tris-HCl pH7.4, 500mM NaCl, 1mM EDTA, 1% Triton x-100) was used for cell lysis and washes.

2.4 Cell culture and retroviral transduction

Murine NIH-3T3 cells were cultured in monolayers in DMEM, 10% FBS, 100 U/mL penicillin/streptomycin, at 37°C and 5% CO_2. Cells were subjected to 2 rounds of virus infection at 10 hour intervals. Infection was monitored by GFP expression by flow cytometry (GUAVA EasyCyte Plus [Millipore]). Extracts were also resolved by SDS-PAGE, transferred to PVDF membrane (Millipore) and protein expression confirmed by Western analysis using anti-eIF4E (BD sciences) and M2 anti-FLAG (Sigma-Aldrich) antibodies. Antibodies were stripped from the membrane by washing 2 x 5min in stripping buffer (1.5% glycine, 0.1% SDS, 1% tween 20, pH 2.2 HCl), 2 X 10 min with PBS (Wisent Inc.), and 2 x 5 min in TBST (0.88% NaCl, 0.1 % Tween 20) before re-probing.

2.5 ^{35}S-Methionine Metabolic labeling

For metabolic labeling, cells were grown to 75% confluency, at which point they were washed once with PBS and incubated in methionine-free DMEM supplemented with 10% dialyzed FBS and 500uCi of ^{35}S-Protein Labeling Mix (Perkin Elmer) for 4h at 37^{o}C. Cells were then washed with cold PBS, two

millimeters of cold PBS added to cover the cells, and the cells were exposed to UV light as described previously (see section 2.2) for 20 min on ice. At this point, cells were lysed with RIPA (anti-eIF4E antibody) or FLAG lysis buffer (M2 anti-FLAG antibody) supplemented with 0.25mM PMSF and 5ug/ml each of aprotinin and leupeptin. Protein concentration was measured using the DC protein assay kit (Bio-Rad). Equal amounts of lysates were pre-cleared with Protein A Sepharose or Protein G Sepharose and the protein of interest immunoprecipitated as described earlier (section 2.3) with anti-eIF4E or anti-FLAG. Laemmli buffer was added and samples resolved by SDS-PAGE. The gel was fixed with 45:45:10 H_2O:methanol:acetic acid overnight, treated with En^3Hance (Perkin Elmer) for 1 h, then water for 1 h, dried and exposed on X-OMAT X-ray film (Kodak). In separate experiments, samples were transferred to PVDF (Millipore) after SDS-PAGE and Western blots performed using anti-eIF4E (BD sciences) and anti-FLAG (Sigma-Alrich) antibodies.

For cytoplasmic extracts, cells were lysed for 15 min at 4^oC with cytoplasmic lysis buffer (50mM Tris-$HCl_{7.5}$, 0.5 % Triton X-100, 137.5 mM NaCl, 10% glycerol) supplemented with proteinase inhibitors. Lysates were centrifuged at 800xg for 5 min at 4^oC. The supernatant was collected and diluted with FLAG lysis buffer. Immunoprecipitations were performed as described above.

2.6 Expression of recombinant protein and m^7-GTP binding assay.

Recombinant FLAG-eIF4E and corresponding mutants were cloned into pET-15b (NcoI/BamHI) and expressed in BL21-codonPlus *E. coli*. Once cultures reached an OD_{600} of 1.0, protein expression was induced with 0.3 mM IPTG for 4 hours at 30°C. Cells were pelleted and resuspended in sonication buffer (0.1M KCl; 20mM $HEPES_{7.5}$, 0.2 mM $EDTA_{8.0}$, 0.5 mM PMSF, 0.5% NP-40). Bacteria were sonicated on ice (nine pulses of 20 seconds at a power setting of 50%, using a Fischer Scientific Membrane dismembrator). Lysates were clarified by centrifugation, once at 1500 x g for 10 min and once at 20,000 x g for 20 min. The cleared lysates were then incubated overnight at 4°C with 50 μL of 50% 7-methyl-GTP Sepharose (GM Healthcare) end-over-end. On the next day, the eIF4E pulldowns were then washed 3 times with 1 mL of sonication buffer.

A binding assay between eIF4E and eIF4G or 4E-BP1 was performed as described previously[91] (see figure 11 for schematic representation of method). Essentially, the eIF4E pulldowns were incubated in binding buffer (20 mM $Tris_{7.5}$, 100 mM KCl, 10% glycerol, and 0.1% NP-40) with either recombinant GST-$eIF4GI_{517-606}$ and GST-4E-BP1 at room temperature for 2 hours and end-over-end rotation. Beads were washed 3 times with 1 mL binding buffer, once with 200µM GDP and eluted with an equal volume of m^7-GTP for 10min each. Fractions of the supernatant, first wash, GDP wash and m^7-GTP elution were resolved on gel, transferred on PVDF membrane (Millipore) and analyzed by Western Blot with anti-eIF4G (Santa Cruz), anti-4E-BP1 (Cell Signaling) and/or anti-eIF4E (BD Sciences) antibodies.

CHAPTER 3: RESULTS

3.1 Cross-linking and immunoprecipitation of eIF4E to mRNA *in vitro*

Commercial anti-eIF4E antibodies, A301-153A (Bethyl) and RN001P (MBL) are being sold with the claim that they can be used for CLIP. We therefore tested to assess if they could immunoprecipitate eIF4E and if other cellular proteins would also be immunoprecipitated with these antibodies (Figure 6). Immunoprecipitation with these antibodies was performed using purified recombinant His_6-eIF4E protein and IPs analyzed by Western blotting for eIF4E. The A301-153A antibody could immunoprecipitate His_6-eIF4E (Figure 6A, lane 7). Antibodies to the His-tag were used in IPs as a positive control (Figure 6A, see lane 6). There was no immunoprecipitation of eIF4E in the IgG non-immune control (Figure 6A, lane 5). A reduction in eIF4E was detected in the supernatant which had been treated with anti-His or A301-153A antibodies, but was absent from the supernatant exposed to IgG (Figure 6A, compare lanes 3 and 4 to 2). Similar results were obtained with the MBL antibody, RN001P (Figure 6B). We conclude that the available commercial antibodies can efficiently immunoprecipitate recombinant His_6-eIF4E.

We then sought to determine if an eIF4E-RNA complex could be immunoprecipitated with these reagents. A short CAT RNA (60 nucleotides) with a ^{32}P labeled cap was cross-linked by UV treatment *in vitro* and immunoprecipitated with the anti-eIF4E antibody, RN001P (MBL) (Figure 7A). As a negative control, the immunoprecipitations were performed from samples

that had not been treated with UV light. Autoradiography of the resolved IPs revealed a UV specific band at the predicted molecular weight of the eIF4E-RNA complex (Figure 7A, lane 4). The molecular weight of this complex also changes upon treatment with RNAse A (Figure 7A, compare lane 6 to 4). We do not observe complete loss of the radioactive signal and attribute this to the cap binding region of eIF4E partially protecting the 5' terminus of the RNA from complete RNase degradation. Immunoprecipitation of these complexes were UV-dependent since they were not present if samples were not exposed to UV light (Figure 7A, compare lane 2 to 4). These complexes (Figure 7A, lane 4 and 6) were also specific to the anti-eIF4E antibody since they were not present in the IgG immunoprecipitates (Figure 7, compare lane 4 to 3 and 6 to 5). Western analysis of the same samples revealed that eIF4E was successfully isolated in all cases where anti-eIF4E was used (Figure 7B, see lane 8, 10 and 12). The higher band representing the eIF4E-RNA complex detected by autoradiography could not be detected by Western Blot, consistent with low efficiency of UV crosslinking and that the eIF4E-RNA species representing a minor proportion of the total amount of eIF4E[xcii].

The same experiment was performed to assess whether mRNA binding to eIF4E was specific for the cap structure. m^7GDP was added as a competitor to eIF4E-cap binding during the pre-incubation period before UV treatment. Following crosslinking and immunoprecipitation, less eIF4E-RNA complex was detected when m^7GDP was present during the UV treatment (Figure 7C compare lane 8 to 7). Consistent with the RNA crosslinking specifically to eIF4E,

unmethylated capped RNA was not crosslinked to eIF4E (Figure 7C, compare lane 3 to 7). This suggests that RNA crosslinking to eIF4E is specifically bound via the m^7GpppN cap structure. As previously shown, IP of the eIF4E-RNA complex is dependent on UV treatment (Figure 7C, compare lane 7 to 6).

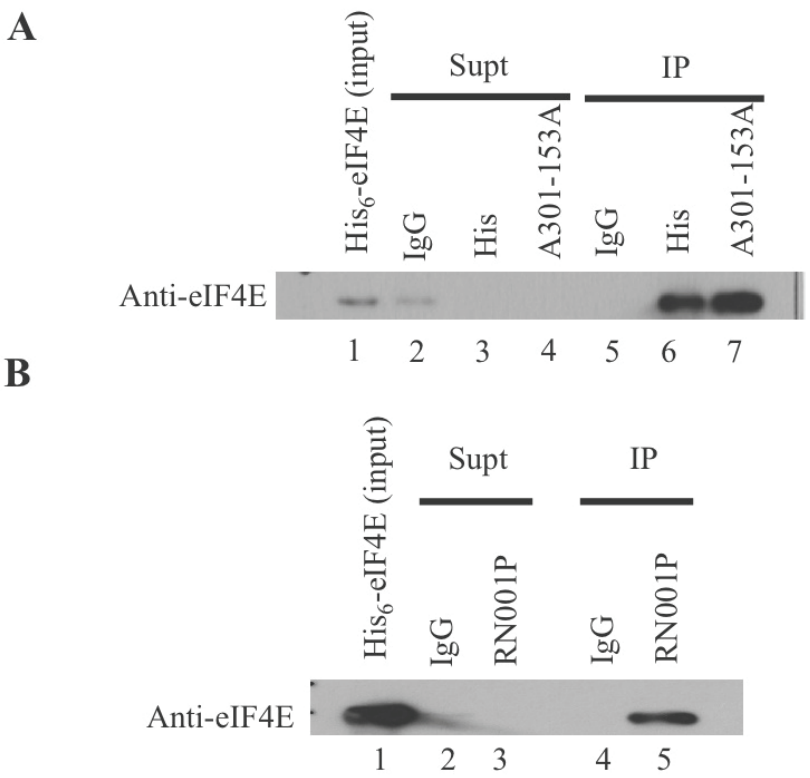

Figure 6: Commercial antibodies were tested for immunoprecipitation.

A. Recombinant His_6-eIF4E was immunoprecipitated with a commercial anti-eIF4E antibody A301-153A (Bethyl), anti-His (positive control) or IgG (negative control) antibodies. IP and supernatant were separated by SDS-PAGE and analyzed by Western Blot. Input is the purified protein directly loaded on gel. Antibody used is shown at the top of the panel. **B**. Recombinant His_6-eIF4E (his-4E) was immunoprecipitated with a commercial anti-eIF4E (RN001P) antibody or IgG from MBL. IP and supernatant were analyzed by Western Blot.

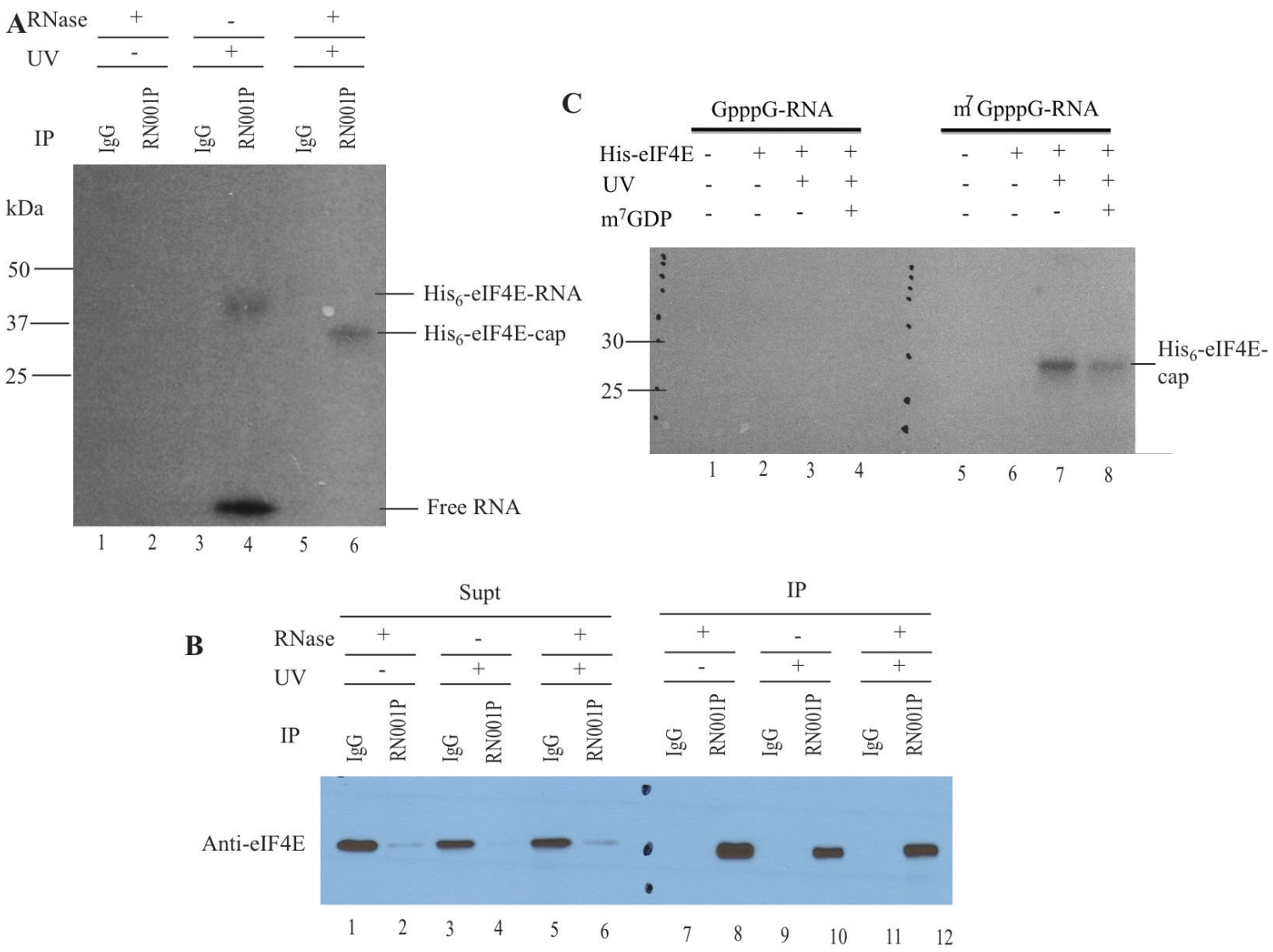
A
RNase + - +
UV - + +
IP IgG RN001P IgG RN001P IgG RN001P
kDa
50
37
25
His6-eIF4E-RNA
His6-eIF4E-cap
Free RNA
1 2 3 4 5 6
C
GpppG-RNA
m7GpppG-RNA
His-eIF4E - + + + - + + +
UV - - + + - - + +
m7GDP - - - + - - - +
30
25
His6-eIF4E-cap
1 2 3 4 5 6 7 8
B
Supt
IP
RNase + - + + - +
UV - + + - + +
IP IgG RN001P IgG RN001P IgG RN001P IgG RN001P IgG RN001P IgG RN001P
Anti-eIF4E
1 2 3 4 5 6 7 8 9 10 11 12

Figure 7: eIF4E crosslink to RNA *in vitro.*

A. Recombinant eIF4E was incubated with ^{32}P-cap-labeled CAT RNA (60 nucleotides) in eIF4E binding buffer**.** Samples were then exposed to UV light at 4^{O}C for 15 min to induce crosslink of eIF4e-RNA complexes. IP was then performed using anti-eIF4E antibody, RN001P, or non-immune IgG from MBL and resolved on a 12% SDS-PAGE and visualized by autoradiography. The lower band seen in the non-RNAse A treated IP (see lane 4) is likely free RNA. **B**. Western Blot of immunoprecipitated samples from the experiment presented in (A) using anti-eIF4E antibody from BD sciences. Both supernatant and IP are shown. UV or RNase A treatment are indicated at the top of the panel. **C.** Recombinant eIF4E was incubated with ^{32}P-m^{7}GpppG or ^{32}P-GpppG 5' labeled CAT RNA in eIF4E binding buffer in the presence or absence of 20μM m^{7}GDP. Samples were exposed to UV light, treated with RNase A and IP performed using the anti-eIF4E from MBL, RN001P. Samples were visualized by autoradiography. UV treatment, the presence of His_6-eIF4E, and/or 20μM m^{7}GDP are indicated at the top of the panel.

3.2 Immunoprecipitation with anti-eIF4E antibodies: specificity and optimization

Given the importance of antibody specificity for CLIP (section 1.12), the specificity of the anti-eIF4E antibodies (RN001P and A301-153A) for immunoprecipitation was tested using S^{35} labeled human 293T cell lysates (Figure 8). In each case, IP with IgG was used as a negative control. For each IP, aliquots were resolved by SDS-PAGE, transferred onto PVDF and Western Blots performed with anti-eIF4E (Bottom Panel in Figure 8A and B, see lane 4), which confirmed successful immunoprecipitation of eIF4E in each case. The upper band in each IP is the mouse anti-eIF4E heavy chain (IgH) used in the IP.

IP samples were also resolved by SDS-PAGE and proteins visualized by autoradiography. The results indicated that eIF4E was enriched upon IP, but also revealed the presence of multiple non-specific proteins (Figure 8A for A301-153A antibody, compare lane 4 to 3) (Figure 8B for RN001P, compare lane 4 to 3**)** despite the presence of detergents (1% NP-40, 1% sodium deoxycholate, 0.1% SDS) in the wash buffer. We attempted to improve the stringency of the IP by using higher NaCl concentrations (500 instead of 150 mM), pre-blocking Sepharose A beads and pre-adsorbing the extract (Figure 8C, compare 4 to 3). Specificity was only slightly improved and we noted significant contamination from unrelated proteins. A comparison between the IP with the anti-eIF4E and with the negative control IgG seems to indicate that even more non-specific proteins were present when anti-eIF4E was used as the precipitating antibody

(Figure 8C, compare 3 to 4). We doubt that the presence of the higher molecular weight proteins were due to co-IP through eIF4E binding given the stringency of the washes, the absence of enrichment of clearly identifiable known binding partners of eIF4E [e.g.- 4E-BP1 (15-20 kDa), eIF4A (50 kDa)]. These results indicate that the commercially available anti-eIF4E antibodies are not sufficiently specific for eIF4E to be used in CLIP assay.

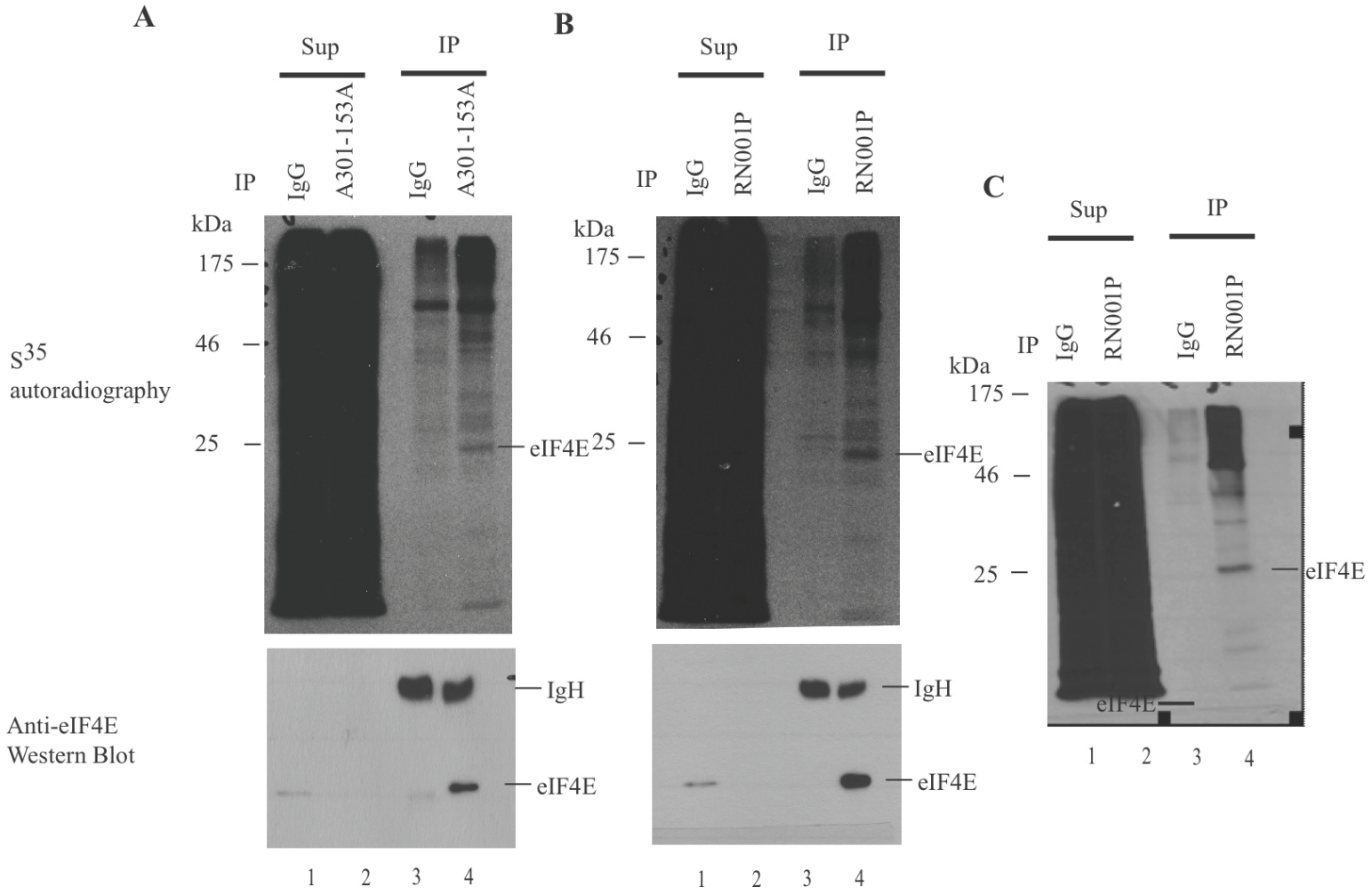
A
Sup
IP
IP
IgG
A301-153A
IgG
A301-153A
kDa
175
46
25
eIF4E
S35
autoradiography
IgH
eIF4E
Anti-eIF4E
Western Blot
1
2
3
4
B
Sup
IP
IP
IgG
RN001P
IgG
RN001P
kDa
175
46
25
eIF4E
IgH
eIF4E
1
2
3
4
C
Sup
IP
IP
IgG
RN001P
IgG
RN001P
kDa
175
46
25
eIF4E
eIF4E
1
2
3
4

Figure 8: Anti-eIF4E antibodies are of poor quality for use in CLIP.

A. Confluent 293T cells were labeled with 500uCi S^{35}-methionine for 4 hours (Perkin Elmer). Cells were lysed with RIPA buffer and clarified by centrifugation. Lysates were immunoprecipitated with anti-eIF4E antibody [A301-153A (Bethyl)], or IgG and washed 4 times with RIPA buffer. The IP and supernatant were resolved on a 12 % SDS-PAGE gel. The gel was fixed, dried and proteins visualized by autoradiography (top). A Western blot was also performed with fractions of the IP and cell supernatant (bottom). **B**. Autoradiography and immunoblot of the IP using anti-eIF4E antibody, RN001P, and performed as in (A) **C.** Immunoprecipitation performed under higher stringency did not eliminated contamination by endogenous cellular proteins. Aliquots from the supernatant and IP were fractionated on a 12 % SDS-PAGE. The IP was performed as in (A) but Sepharose beads were pre-blocked with 5% BSA. Also, lysis and washes with RIPA contained 0.5M NaCl. Lysates were pre-cleared before performing the IP by incubating with Sepharose A beads before the IP.

3.3 FLAG-eIF4E

Given the above mentioned results, we sought to use an amino-terminal FLAG tagged eIF4E in the hope of being able to perfrom more stringent IPs. The FLAG tag was chosen because it is routinely used in CHIP-seq[93], has successfully been used in the CLIP assay in the past[94], and eIF4E can tolerate modifications at its N-terminus while retaining function[95]. FLAG-eIF4E was robustly expressed in cells transduced by retroviral infection. A Western blot of non-infected and partially infected cells (30% GFP positive cells by flow cytometry) indicated that FLAG-eIF4E was expressed (Figure 9A). On the Western Blot with anti-eIF4E, endogenous eIF4E (bottom) was detected at 25 kDa and FLAG-eIF4E (top) could be seen at a higher molecular weight, consistent with its predicted size being 28kDa. FLAG-eIF4E was also detected when immunoblotted with anti-FLAG.

Immunoprecipitation of S^{35} labeled lysates from uninfected or MSCV/FLAG-eIF4E infected cells was performed, followed by size separation on SDS-polyacrylamide gel. Western blotting using anti-eIF4E antibodies confirmed that the IPs with the anti-FLAG antibody (Figure 9B, compare lane 2,3 to lane 1) were successful. When IPs were visualized by autoradiography, immunoprecipitations using anti-FLAG antibodies enriched for a specific protein between 25 - 30 kDa and present in cells infected with MSCV/FLAG-eIF4E, but not from uninfected cells (Figure 9C, compare lanes 2 and 3 to 1). This is consistent with this protein being FLAG-eIF4E (expected size of 28 kDa). The same protein was also immunoprecipitated from cells that had been treated with UV-light (Figure 8C, see lane 5 and 6).

A second protein species, having a molecular weight >175 kDa was also present in the IP from MSCV/FLAG-eIF4E extracts. It is unlikely that this protein is enriched because it cross-reacts with anti-FLAG antibodies since it is not present in the anti-FLAG IP from uninfected cells (Figure 9C, compare lane 1 to 2). One explanation is that this protein was co-immunoprecipitated because it associated with recombinant FLAG-eIF4E. As such, one possibility is that it represents eIF4G (~220 kDa) given its apparent high molecular weight. We address this point below with an eIF4E mutant that does not interact with eIF4G (section 3.4). Increasing the stringency of the washes by increasing the NaCl from 150 mM to 500 mM reduced the background levels of co-precipitating proteins (compare lane 3 to 2). These results indicate that using an anti-FLAG antibody yielded much cleaner IPs than we could obtain with the commercially available anti-eIF4E antibodies. Subsequent pilot experiments utilized the anti-FLAG antibodies.

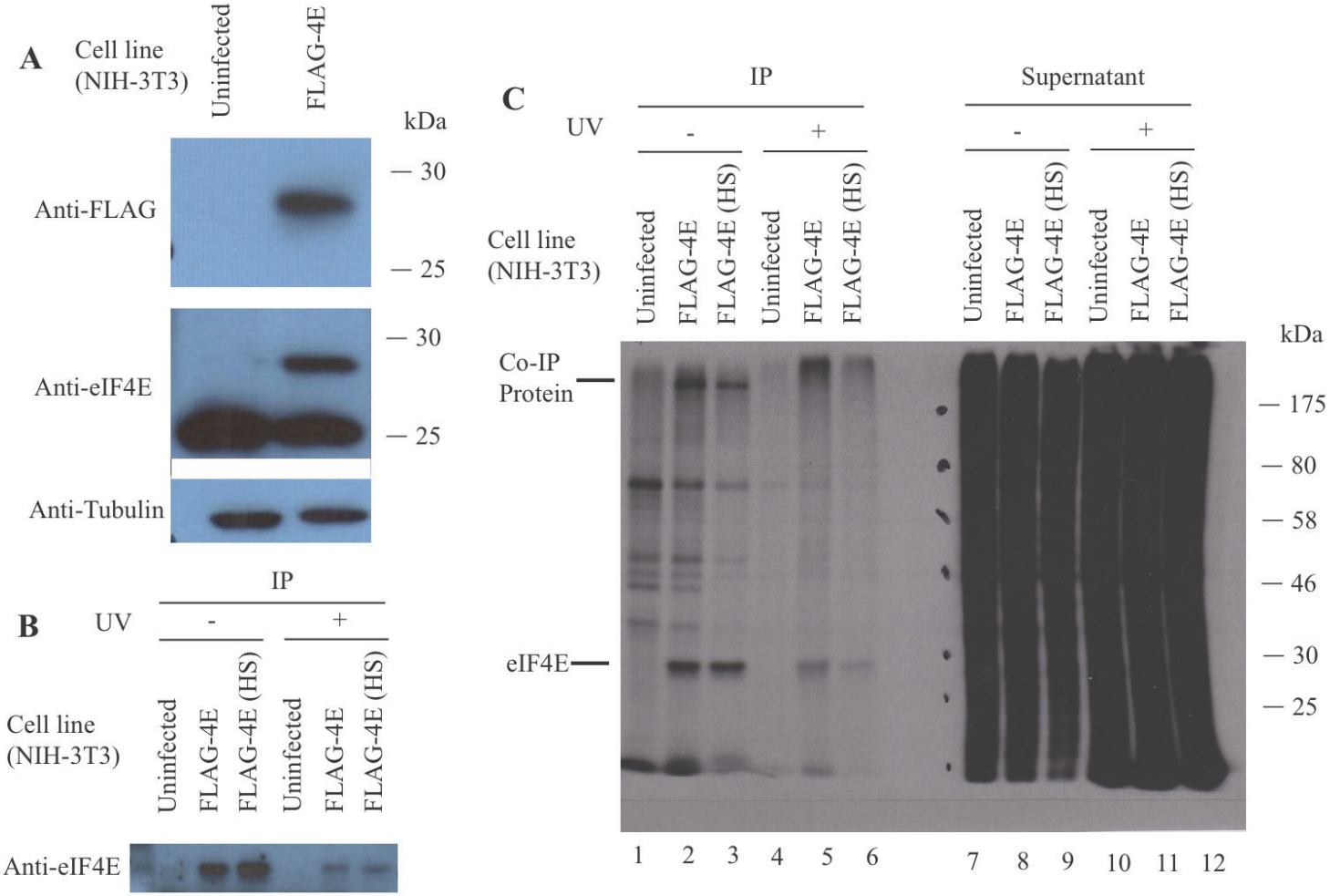
A
Cell line
(NIH-3T3)
Uninfected
FLAG-4E
kDa
Anti-FLAG
— 30
— 25
Anti-eIF4E
— 30
— 25
Anti-Tubulin
B
UV
IP
-
+
Cell line
(NIH-3T3)
Uninfected
FLAG-4E
FLAG-4E (HS)
Uninfected
FLAG-4E
FLAG-4E (HS)
Anti-eIF4E
C
UV
IP
Supernatant
-
+
Cell line
(NIH-3T3)
Uninfected
FLAG-4E
FLAG-4E (HS)
Co-IP
Protein
eIF4E
kDa
— 175
— 80
— 58
— 46
— 30
— 25
1 2 3 4 5 6 7 8 9 10 11 12

Figure 9: Immunoprecipitation of FLAG-eIF4E .

A. Extracts from uninfected NIH-3T3 and MSCV/FLAG-eIF4E infected NIH-3T3 cells, prepared for Western blotting and probed with anti-eIF4E, anti-FLAG and anti-tubulin antibodies. **B.** Uninfected NIH-3T3 and MSCV/FLAG-eIF4E infected NIH-3T3 were incubated with 500uCi of S^{35}-methionine/cysteine and lysed with FLAG lysis buffer. Lysates were pre-cleared using Protein G Sepharose and anti-FLAG (M2) antibody was used in IP reactions. The IP were resolved by SDS-PAGE and a Western Blot was performed. In lanes marked with (HS), 500mM NaCl was used for IP (lane 3 and 6**). C.** IP and Supernatant from the immunoblot shown in (B) were resolved by SDS-PAGE and visualized by autoradiography.

A

```
1   ggaggcggag ggagctggtc cttaaggaag gcacgcgctt gcttctagat tccgaagcgt
                  M  A  T  V  E  P  E  T  T  P  T  T  N  P  P  P
61  tttcaaagct ggttacagtc cttaccacag cacacccttg tgaggagcgg ttgtgcgatc
121 agatcgatct aagatggcga ctgtggaacc ggaaaccacc cctaccacta atccccccacc
     A  E  E  E  K  T  E  S  N  Q  E  V  A  N  P  E  H  Y  I  K
181 tgcagaagag gaaaaaacag agtctaatca ggaggttgct aacccagagc actatattaa
     H  P  L  Q  N  R  W  A  L  W  F  F  K  N  D  K  S  K  T  W
241 acaccctcta cagaacaggt gggcactctg gttttttaaa aatgataaaa gcaaaacttg
     Q  A  N  L  R  L  I  S  K  F  D  T  V  E  D  F  W  A  L  Y
301 gcaagcaaac cttcgattga tctctaagtt tgatactgtt gaagactttt gggctctata
     N  H  I  Q  L  S  S  N  L  M  P  G  C  D  Y  S  L  F  K  D
361 caaccatatc cagttgtcta gtaatttaat gcctggctgt gactactcac tttttaagga
     G  I  E  P  M  W  E  D  E  K  N  K  R  G  G  R  W  L  I  T
421 cgggattgag cctatgtggg aagatgagaa aaacaaacga ggaggacggt ggctgatcac
     L  N  K  Q  Q  R  R  S  D  L  D  R  F  W  L  E  T  L  L  C
481 actgaacaag cagcagagac ggagtgacct cgatcgcttc tggctagaga cactgctgtg
     L  I  G  E  S  F  D  D  Y  S  D  D  V  C  G  A  V  V  N  V
541 ccttattgga gaatctttcg atgactacag tgatgatgtg tgtggagctg ttgttaatgt
     R  A  K  G  D  K  I  A  I  W  T  T  E  C  E  N  R  D  A  V
601 tagagctaaa ggtgataaga tagcaatatg gactactgag tgtgaaaaca gagatgcagt
     T  H  I  G  R  V  Y  K  E  R  L  G  L  P  P  K  I  V  I  G
661 cacacacata gggagggtat acaaggaaag gttaggactt cctccgaaga tagtgattgg
     Y  Q  S  H  A  D  T  A  T  K  S  G  S  T  T  K  N  R  F  V
721 ttatcagtcc cacgcagaca cagctacaaa gagcggctcc accactaaaa ataggtttgt
     V  *
781 tgtttaagaa gacaccttct gagtattctc acaggagact gcgtcacgca atcgagattg
841 ggagctgaac caaagcctca tcaaagcaga gtggactgca ctgaagttga ttccatccaa
```

B

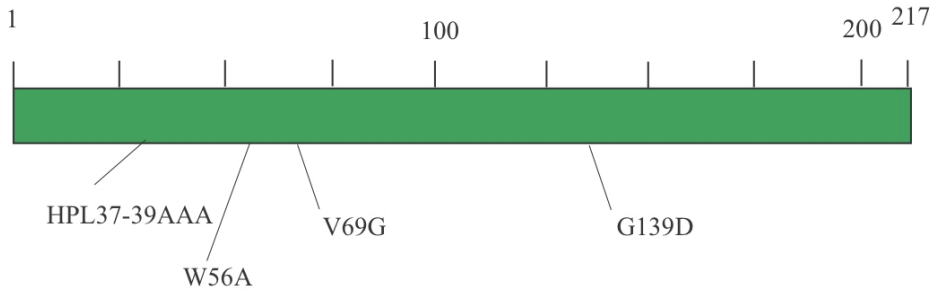

Figure 10: EIF4E mutations.

A The letters in red represents point mutations that were made by PCR using the murine cDNA as template. The eIF4E(W56A) mutant can still interact with other initiation factors and assemble into the eIF4F but cannot bind mRNA. The HPL37-39AAA, V69G and G139D mutants were identified in a yeast screen to have impaired binding to eIF4G. **B.** Relative position of the eIF4E mutations.

3.4 The eIF4E(G139D) mutant binds the cap but not eIF4G

To control for non-specific interactions with RNA that could occur during the different steps of the CLIP process, we decided to generate an eIF4E mutant that could serve as a negative control. eIF4E(W56A) harbors a mutation at a conserved tryptophan residue in the cap binding pocket to alanine (Figure 10). This abolishes its cap recognition (see section 1.2) and mRNA binding properties. Such a mutant is an ideal negative control for CLIP. Secondly, since eIF4E is a subunit of eIF4F and associates with eIF4G (Figure 2), a mutant that could uncouple eIF4E interaction with eIF4G (and 4E-BP1) could be quite useful in determining if there are subsets of mRNAs that interact with free eIF4E versus eIF4F-complexed eIF4E. To this end, a previously described mutant eIF4E (W73A) would appear quite useful since this mutant has been reported to be incapable of interacting with eIF4G[96]. However, the eIF4E(W73A) mutant is very unstable in cells and is rapidly degraded by ubiquination when ectopically expressed in cells[96]. Hence, it is not useful for the proposed CLIP studies.

We therefore decided to generate and test a series of previously described yeast mutants that had been identified to lack eIF4G/4E-BP1 binding using a yeast two hybrid system[97] (HPL37-39AAA, V69G and G139D) (Figure 10). We engineered these mutants into the murine eIF4E cDNA, engineered a FLAG tag, and purified the recombinant protein from *E.coli*. The recombinant proteins were tested for their ability to bind m^7GTP and to interact with GST-eIF4GI$_{517\text{-}606}$. A schematic representation of the assay used and the expected results are shown in

figure 11. The wild-type FLAG-eIF4E, used as a positive control in these experiments, was specifically pulled down by the m^7GTP cap affinity column and bound to GST-eIF4GI$_{517-606}$ (Figure 12B, see lane 1) and GST-4E-BP1 (Figure 12C, see lane 1). Of all the mutants screened, only FLAG-eIF4E(G139D) showed appreciable cap binding activity (Figure 12A, compare lane 5 to 2,3 and 4). The FLAG-eIF4E(V69G) and FLAG-eIF4E(HPL) were unable to bind to the cap affinity resin (Figure 12A, see lane 2 and 4).

Pulldown of recombinant GST-eIF4GI$_{517-606}$ or GST-4E-BP1 with recombinant eIF4E mutants immobilized on m^7GTP cap affinity column were performed as shown in Figure 11. Samples were extensively washed, resolved on a 10% polyacrylamide gel and analyzed by Western blot. The FLAG-eIF4E(G139D) mutant was severely impaired for GST-eIF4GI$_{517-606}$ and GST-4E-BP1 binding while a significant amount of GST-eIF4GI$_{517-606}$ /GST-4E-BP1 was pulled down by m^7GTP-immobilized FLAG-eIF4E (Figure 12B and C, compare lane 2 to 1). eIF4E, GST-eIF4GI$_{517-606}$ and GST-4E-BP1 were only recovered in m^7GTP eluents and not GDP or binding buffer washes (Figure 12B and C, compare lane 1 and 2 to 3,4,5 and 6). This showed that pulldown of GST-eIF4GI$_{517-606}$ and GST-4E-BP1 were specific for eIF4E and that FLAG-eIF4E(G139D) can bind the cap structure but does not bind eIF4G or 4E-BP1 *in vitro*.

The FLAG-eIF4E, FLAG-eIF4E(W56A) and FLAG-eIF4E(G139D) cDNAs were cloned into MSCV and transduced in NIH 3T3 cells. Cells expressing FLAG-eIF4E, FLAG-eIF4E(W56A) and FLAG-eIF4E(G139D) were

labeled with S^{35}-methionine/cysteine. From these, cytoplasmic extracts were prepared and immunoprecipitated with anti-FLAG antibody (Figure13A). As expected, the high molecular weight band (Figure 13A, compare lane 3 to 1, see protein A) is immunoprecipitated with FLAG-eIF4E, but not with FLAG-eIF4E(G139D), suggesting that this protein is eIF4G. Other specific bands were also immunoprecipitated with FLAG-eIF4E, but not FLAG-eIF4E(G139D) (Figure 13A, compare lane 1 to 3). Given their molecular weight we suspected them to be eIF4B or PABP (Figure 13A, protein B), eIF4A (Figure 13A, protein C) and 4E-BP1, (Figure 13A, protein D). The identities of 4E-BP1 and eIF4AI (lower band) were confirmed by Western blotting (Figure 13B). We have not yet confirmed the identity of proteins labeled A or B.

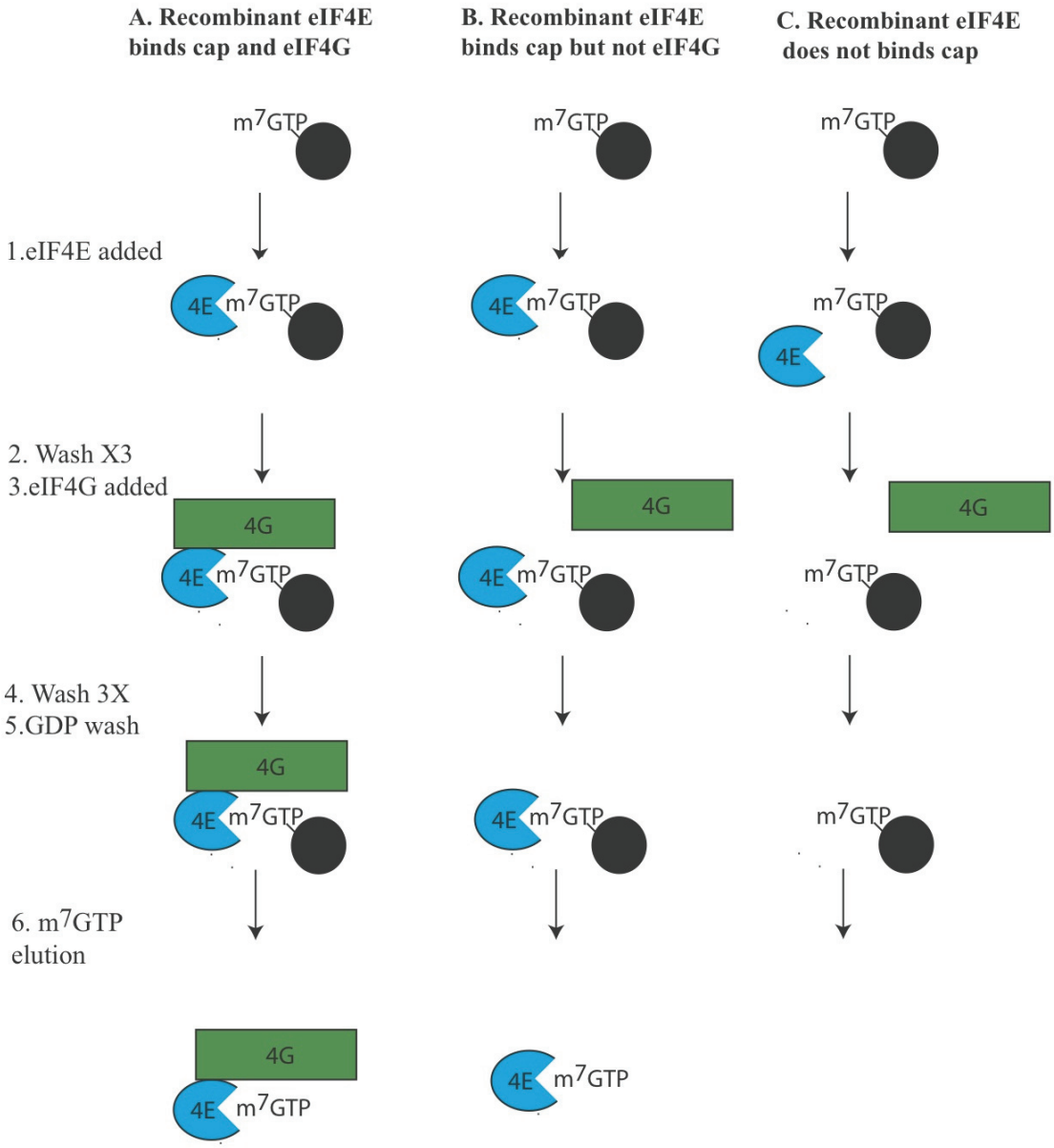
A. Recombinant eIF4E binds cap and eIF4G
B. Recombinant eIF4E binds cap but not eIF4G
C. Recombinant eIF4E does not binds cap
m7GTP
1.eIF4E added
4E
2. Wash X3
3.eIF4G added
4G
4. Wash 3X
5.GDP wash
6. m7GTP elution

Figure 11: Schematic representation of pulldown assays used with the eIF4E mutants.

A. If the eIF4E (wild type or mutant) can bind the cap structure (m^7GTP) and GST-eIF4GI$_{517-606}$ (4G), both will be recovered upon m^7GTP elution from m^7GTP-agarose beads (shown at the top of the figure as black circles linked to m7GTP). **B**. If the eIF4E can bind the cap structure but has impaired eIF4G binding ability, only eIF4E will be recovered. **C**. If the mutant has no cap binding activity, no protein will be recovered.

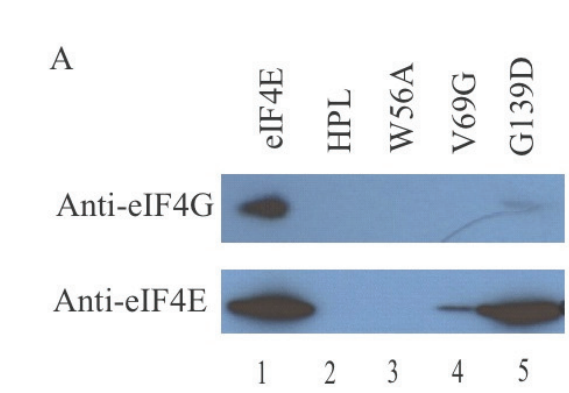
A
eIF4E
HPL
W56A
V69G
G139D
Anti-eIF4G
Anti-eIF4E
1 2 3 4 5

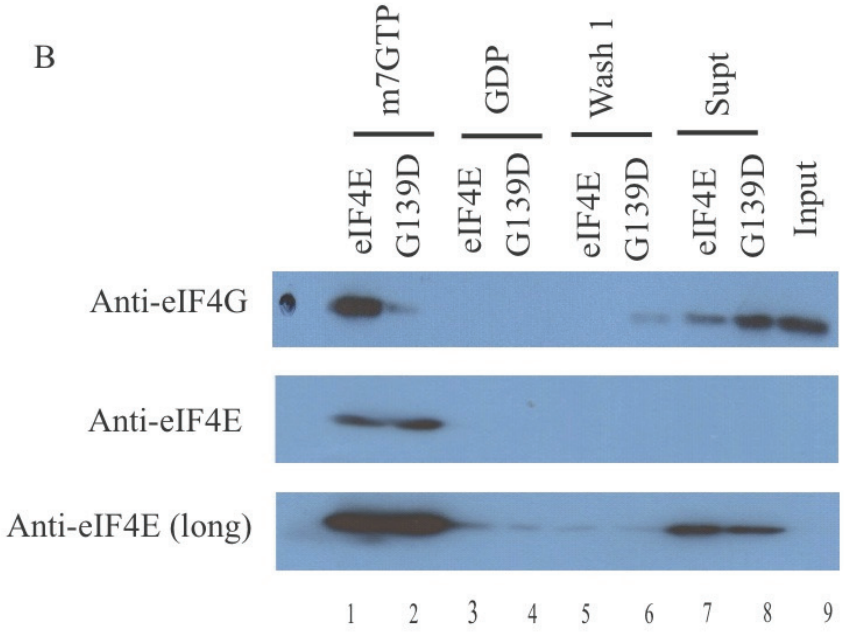
B
m7GTP
GDP
Wash 1
Supt
eIF4E
G139D
Input
Anti-eIF4G
Anti-eIF4E
Anti-eIF4E (long)
1 2 3 4 5 6 7 8 9

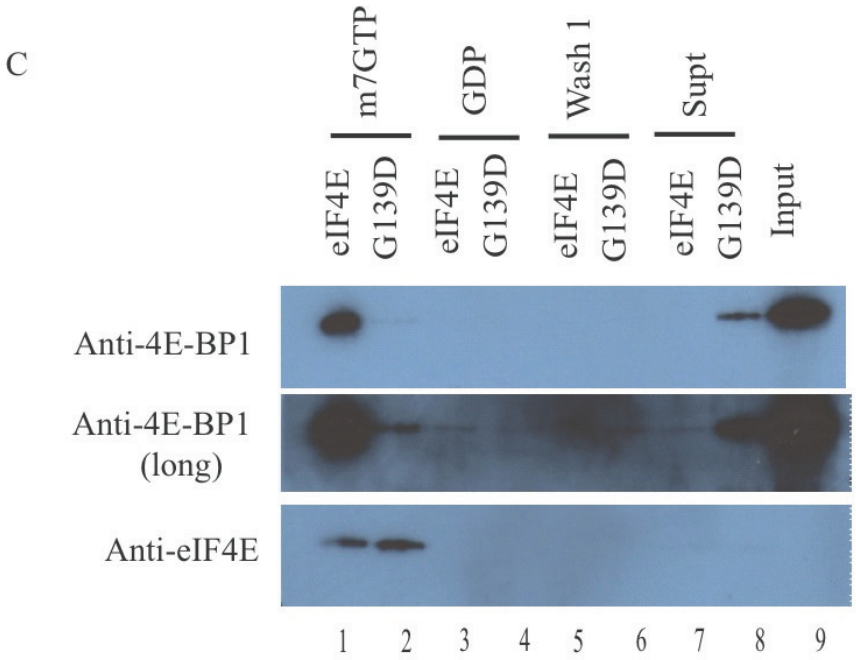
C
m7GTP
GDP
Wash 1
Supt
eIF4E
G139D
Input
Anti-4E-BP1
Anti-4E-BP1
(long)
Anti-eIF4E
1 2 3 4 5 6 7 8 9

Figure 12: FLAG-eIF4E(G139D) can bind the cap but not GST-eIF4GI$_{517-606}$ or GST-4E-BP1.

A. Assessing cap binding of FLAG tagged eIF4E (eIF4E) and mutant eIF4Es (HPL, W56A, V69G, G139D) by retention on m^{7}GTP-Sepharose. Bacterial lysates prepared from each mutant were purified by m^{7}GTP affinity chromatography. m^{7}GTP-Agarose bound FLAG-eIF4E mutants were used to pull down GST-eIF4GI$_{517-606}$ and m^{7}GTP (0.2mM) eluents were analyzed by Western Blot. **B.** Comparison of the ability of FLAG-eIF4E (WT) and FLAG-eIF4E(G139D) to interact with GST-eIF4GI$_{517-606}$. Pulldown of GST-eIF4GI$_{517-606}$ with m^{7}GTP-immobilized FLAG-eIF4E (WT) and FLAG-eIF4E (G139D) were performed as in (A) and were washed with GDP before elution with m^{7}GTP and analysis by Western Blot. Immunoblot of m^{7}GTP elution, GDP wash, 1st wash, supernatant and input are presented. **C.** Pulldown of GST-4E-BP1 with m^{7}GTP-immobilized FLAG-eIF4E (WT) and FLAG-eIF4E(G139D) were washed with GDP before elution with m^{7}GTP and analysis by Western Blot. Membranes were blotted using 4E-BP1 antibodies from Santa Cruz.

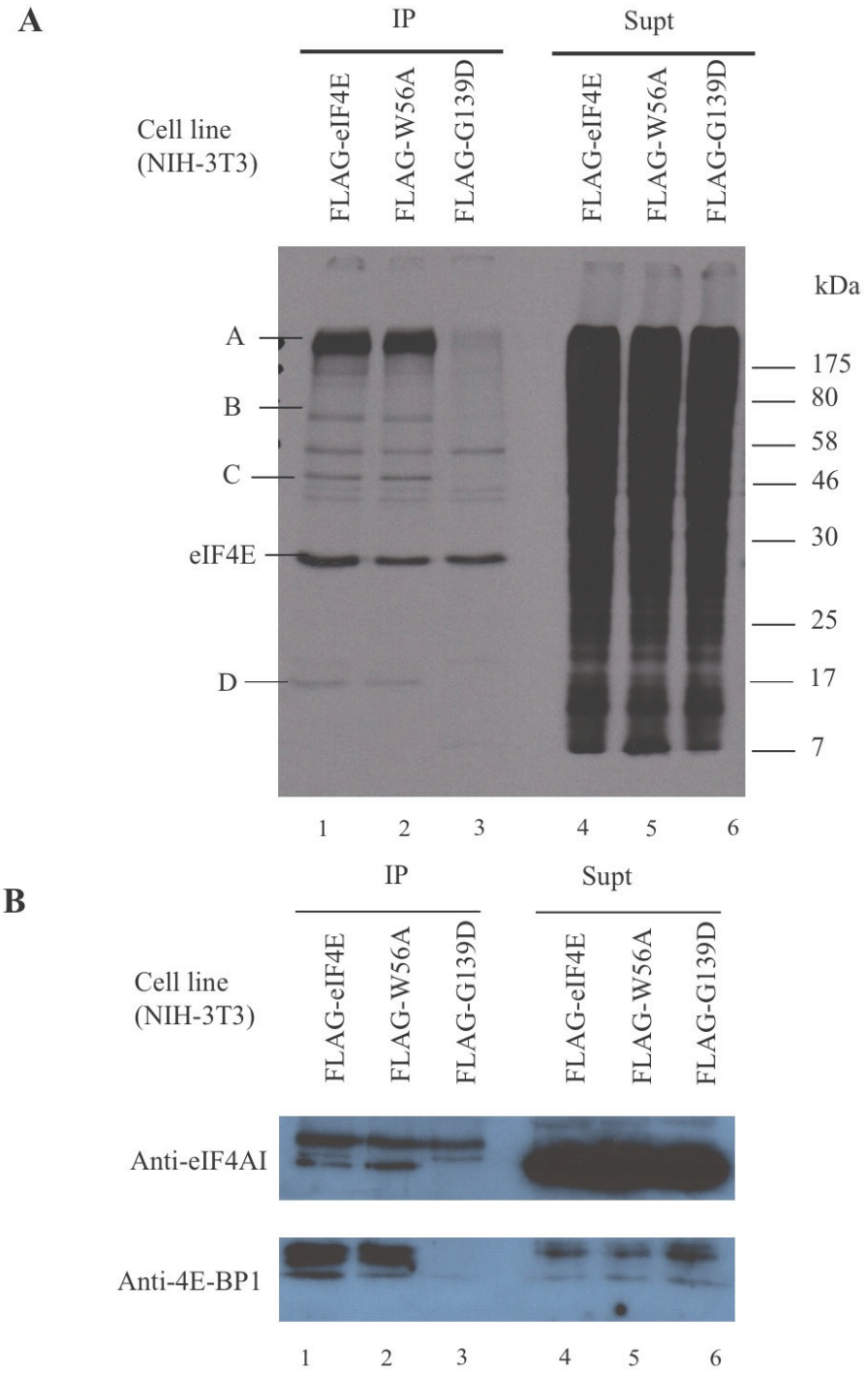
A
IP
Supt
Cell line
(NIH-3T3)
FLAG-eIF4E
FLAG-W56A
FLAG-G139D
FLAG-eIF4E
FLAG-W56A
FLAG-G139D
kDa
A
B
C
eIF4E
D
175
80
58
46
30
25
17
7
1 2 3 4 5 6
B
IP
Supt
Cell line
(NIH-3T3)
FLAG-eIF4E
FLAG-W56A
FLAG-G139D
FLAG-eIF4E
FLAG-W56A
FLAG-G139D
Anti-eIF4AI
Anti-4E-BP1
1 2 3 4 5 6

Figure 13: IP of radiolabeled cytoplasmic extract from cells expressing FLAG-eIF4E(G139D) do not co-immunoprecipitate eIF4G.

A. Immunoprecipitation with anti-FLAG antibody was performed on cytoplasmic extracts from cells radiolabeled with S^{35}-methionine/cysteine expressing FLAG-eIF4E, FLAG-eIF4E(W56A) and FLAG-eIF4E(G139D). Immunoprecipitation and supernatant samples were separated by SDS-PAGE and visualized by autoradiography **B.** Western blot of extracts shown in (A) probed with anti-eIF4AI (Abcam) and anti-4E-BP1 (Santa-Cruz) antibodies.

CHAPTER 4: DISCUSSION

Establishing a direct *in vivo* assay to define the eIF4E-mRNA interactome would prove to be very useful in better understanding the effects of deregulated eIF4E expression and cap-dependent mRNA translation that occurs in different physiological settings, such as cancer and virus infection. The study of eIF4E has been plagued by an absence of robust assays to directly examine eIF4E-mRNA interactions *in vivo*. Our understanding of eIF4E has mainly been the result of indirect observations or by *in vitro* experimentation. Being able to assay eIF4E interactions in a robust manner *in vivo* would be an invaluable tool to better dissect eIF4E biological role in global cellular mRNA translation, its mRNA targets and to screen for eIF4E inhibitors in an *in vivo* setting.

Here we show that we can recapitulate UV cross-linking of eIF4E to mRNA. Once cross-linked, eIF4E seems to protect, at a minimum, the cap structure of RNA from RNAse A degradation as shown by the ever present radioactive signal of the cap after immunoprecipitation and treatment with RNase A (Figure 7A). This binding appears to be specific to the cap structure as predicted by what is known about protein-RNA crosslinking by UV_{254} and revealed by a reduction in signal upon competition with m^7GDP (Figure 7C).

A potential issue observed during the *in vitro* assays is the low efficiency of cross-linking. Although formation of RNA-protein complex could be observed by autoradiography, they could never be observed by Western Blot. There are two possible explanations: the efficiency of cross-linking is very low resulting in

minute amounts of purified eIF4E-RNA or that after crosslinking of eIF4E bound to RNA, the antibody used for immunoblotting can no longer bind its target because of steric hindrance or conformational changes. The former explanation is more likely given the fact that Western Blots were performed with different eIF4E antibodies targeting different regions of eIF4E and all failed to detect an eIF4E-RNA complex. This result is also consistent with what other laboratory have observed when performing CLIP with other proteins[74].

An option to explore in order to increase cross-linking efficiency is performing PAR-CLIP. In this technique, a relatively photoreactive nucleotide analogue such as 4-thioluridine(4-SU) or 6-thioguanosine (6-SG), is added to cells. These nucelotides are used indiscriminately by the cells and incorporated into RNA. Cross-link is accomplished at higher efficiencies with lower energy levels (365nm). The technique has been successfully used with FLAG tagged proteins[98]. One could imagine that cells incubated with 6-SG would readily incorporate the analogue within the cap structure allowing for unbiased cross-linking of mRNA to the cap structure. This though would have to be tested *in vitro* with synthetic RNA and recombinant eIF4E. Also, cross-linking of eIF4E to RNA in high-salt washed ribosome extracts with 4-SU at the +2 position adjacent to the cap has been previously shown to be relatively efficient[99]. One would have to keep him mind that the toxicity of these nucleotides has not been studied in depth when interpreting the data generated from these experiments.

Commercially available eIF4E antibodies were tested for specificity. Our results indicated that these antibodies would not be very useful for CLIP since

they appeared to immunoprecipitate many other proteins in addition to eIF4E. The absence of non-specific immunoprecipitated proteins from the IgG negative control suggests that all the non-specific immunoprecipitation were due to the eIF4E antibodies themselves (Figure 8). We doubt that these are eIF4E-associated proteins given the harsh conditions of IP (1% sodium deoxycholate, 1% NP-40, 0.1% SDS and 500mM NaCl), which should cause dissociation of most protein-protein interactions. We concluded that the commercial antibodies are not sufficiently specific for CLIP.

In order to obtain immunoprecipitations that were significantly more enriched for eIF4E, we engineered a FLAG tag at the N-terminal of eIF4E and stable cell lines expressing FLAG-eIF4E were generated. The FLAG tag is frequently used for CHIP-seq and has shown success with CLIP[94]. Expression of recombinant FLAG-eIF4E was robust and stable. The FLAG-eIF4E construct could bind m^7GTP and interacted with GST-eIF4GI$_{517-606}$ and GST-4E-BP1 (Figure 12) suggesting that it was still functional. Also, immunoprecipitation of cytoplasmic extracts of cells lines expressing the FLAG-eIF4E co-immunoprecipitated several protein species that had molecular weights similar to the known subunits of eIF4F (i.e. eIF4G, eIF4A, PABP), or that interact with eIF4E (i.e. 4E-BP) or eIF4A (i.e. eIF4B) (Figure 13). The identity of eIF4A and 4E-BP1 as associated proteins were confirmed by Western blotting. We suspect that bands A and B are eIF4G and eIF4B (80kDa) or PABP (73kDa), respectively. PABP is known to interact with eIF4G[100] and eIF4B has been shown to interact with eIF4A[99]. Immunoprecipitation with anti-FLAG antibodies indicated that the

IP were very specific and that non-specific pulldown of other proteins is much cleaner than with the commercially available anti-eIF4E antibodies (Figure 13). This said, more experiments to measure the level of non-specific pulldown of RNA still need to be performed.

A series of mutants were generated to test the specificity of eIF4E interactions and make it possible to better dissect free eIF4E function independently from when it is complexed in eIF4F. The eIF4E(W56A) mutant, in which a conserved tryptophan essential for cap binding has been mutated to alanine, has been shown to lack RNA binding activity but can still participate in the formation of the eIF4F complex[101]. This mutant could serve as a very good negative control for CLIP. Elimination of results obtained with this mutant from the results obtained with the wild-type, as well as bioinformatics selection of sequences for only those derived from the 5' end of the transcripts, would permit us to obtain a confident representative dataset of the eIF4E interactome. It would also be desirable to be able to have an eIF4E mutant that does not bind eIF4G since this would allow us to probe between mRNAs that interact directly with free eIF4E versus eIF4F-bound eIF4E. The eIF4E(W73A) mutant was initially designed to not interact with eIF4G[102], but recent studies have indicated it to not be very stable. Indeed, expression of eIF4E(W73A) was barely detectable in cell lines 24 hours after retroviral transduction[103]. For these reasons, we tested a series of eIF4E mutants that had been described in a yeast two-hybrid assay to have reduced interaction with eIF4G and/or 4E-BP1[97,104], but had never been validated with human or murine eIF4E for cap binding affinity.

The eIF4E mutants HPL37-39AAA, V69G, G139D were cloned, expressed in bacteria, purified and tested for cap binding affinity. Of these, only eIF4E(G139D) retained ability to bind the cap structure (Figure 12). The eIF4E(G139D) mutant had also lost the ability to interact with eIF4GI and 4E-BP1 (Figure 12 and 13). When ectopically expressed in cells, the mutant was still detectable after 72 hours, albeit at reduced levels. Also, immunoprecipitation of S^{35} labeled cytoplasmic extract from cells expressing eIF4E (G139) showed a reduction when compared to FLAG-eIF4E in several protein known to be subunits of eIF4F (eIF4G, eIF4A), that interact with eIF4E (4E-BP) which is consistent with the *in vitro* data. More rigorous experimentation exploring the stability of this mutant in cells are needed and are currently in process of being performed (e.g. S^{35}-methionine pulse chase for stability and comparison studies with the eIF4E(W73A) mutant).

Ectopic over-expression of FLAG-eIF4E will be a major concern when attempting to define the eIF4E interactome since this would not be physiologically relevant. There is no doubt that overexpression of eIF4E is driving mRNA translation of transcripts which are not normally highly expressed. There is also evidence of rewiring of downstream targets of the PI3K pathway and dephosphorylation of 4E-BP1 and S6K1 (p70)[105], when eIF4E is overexpressed. Despite the disadvantage of not pulling down endogenous eIF4E, the FLAG tag ensures that immunoprecipitation is specific. To ensure that the results obtained by using a FLAG tag represent physiological settings, a FLAG tag can be engineered in front of the endogenous eIF4E sequence using DNA engineering

approaches. This would ensure that eIF4E levels are at physiological levels and can be specifically immunoprecipitated. A relatively simple and efficient method of editing the genome and adding the FLAG tag would be to use transcription activator-like effector nucleases (TALENS)[106], an option that is currently being pursued.

CHAPTER 5: CONCLUSION

This work sets the groundwork for 4E-CLIP. We concluded from *in vitro* experiments that eIF4E cross-linking to mRNA is specific. We also establish that eIF4E-mRNA complexes can be purified by immunoprecipitation. Despite the minor setback from the lack of commercially available specific and RIP grade eIF4E antibodies, FLAG tags were added to the eIF4E N-terminal domain which allowed for higher specificity during the immunoprecipitation. We also characterized a series of eIF4E mutants for their ability to retain cap-binding ability but harbor impaired eIF4G interaction. Of these, eIF4E(G139D) was found to be a promising candidate.

This work brings up possible methods to improve 4E-CLIP and to better enrich immunoprecipitation of eIF4E-mRNA complexes. The 4E-CLIP technique, once established could serve as a springboard for the development and screen of novel eIF4E inhibitors. It would also be a powerful tool to better understand the role of deregulated eIF4E expression in protein synthesis in tumorigenic cells.

REFERENCES

1. Lodish HF, Berk A, Kaiser C, Krieger M, Scott MP, Bretscher A, Ploegh H, Matsudaira PT. "Chapter 8: Post-transcriptional Gene Control". *Molecular Cell. Biology*. 2007.San Francisco: WH Freeman
2. Kapp LD, Lorsch JR. The molecular mechanics of eukaryotic translation. *Annu Rev Biochem*. 2004; 73:657-704.
3. Gingold H, Pilpel Y. Determinants of translation efficiency and accuracy. *Mol Syst Biol*. 2011 Apr 12;7:481.
4. Shatkin AJ. Capping of eucaryotic mRNAs. *Cell*. 1976 Dec;9(4 Pt 2):645–653.
5. Ogino T, Banerjee AK. An unconventional pathway of mRNA cap formation by vesiculoviruses. *Virus Res*. 2011 Dec; 162(1-2):100-9.
6. Bélanger F., Stepinski J., Darzynkiewicz E. and Pelletier J. Characterization of hMTr1, a Human Cap1 2‘-O-Ribose Methyltransferase . *J. Biol. Chem*. 2010; 285, 33037–33044.
7. Kuge H, Brownlee GG, Gershon PD, and Richter JD. Cap ribose methylation of c-mos mRNA stimulates translation and oocyte maturation in Xenopus laevis. *Nucleic Acids Res*. 1998 July 1; 26(13): 3208–3214.
8. Werner M., Purta E, Kaminska KH, Cymerman IA, Campbell DA, Mittra B, Zamudio JR, Sturm NR, Jaworski J, Bujnicki JM. 2'-O-ribose methylation of cap2 in human: function and evolution in a horizontal mobile family. *Nucl. Acids Res*. 2011, 39, 4756–4768.
9. Varani G. A cap for all occasions. *Structure*. 1997; 5:855–858.
10. Schoenberg DR, Maquat LE. Re-capping the message. *Trends Biochem Sci*. 2009 Sep; 34(9):435-42.
11. Tomoo K, Shen X, Okabe K, Nozoe Y, Fukuhara S, Morino S, Ishida T, Taniguchi T, Hasegawa H, Terashima A, Sasaki M, Katsuya Y, Kitamura K, Miyoshi H, Ishikawa M, Miura K. Crystal structures of 7-methylguanosine 5'-

triphosphate (m(7)GTP)- and P(1)-7-methylguanosine-P(3)-adenosine-5',5'-triphosphate (m(7)GpppA)-bound human full-length eukaryotic initiation factor 4E: biological importance of the C-terminal flexible region. *Biochem J*. 2002 Mar 15; 362(Pt 3):539-44.

12. Matsuo H, Li H, McGuire AM, Fletcher CM, Gingras AC, Sonenberg N, Wagner G. Structure of translation factor eIF4E bound to m7GDP and interaction with 4E-binding protein. Nat Struct Biol. 1997 Sep;4(9):717-24.
13. Sonenberg N, Hershey JWB., Mathews MB. Translational control of gene expression. *Cold Spring Harbor Laboratory Press*. 2000.
14. S. Morino, H. Hazama, M. Ozaki, Y. Teraoka, S. Shibata, M. Doi, H. Ueda, T. Ishida, S. Uesug. Analysis of the mRNA cap-binding ability of human eukaryotic initiation factor-4E by use of recombinant wild-type and mutant forms. *Eur. J. Biochem.*, 1996; 239, pp. 597–601.

15 H. Ueda, H. Iyo, M. Doi, M. Inoue, T. Ishida, H. Morioka, T. Tanaka, S. Hishikawa, S. Uesugi. Combination of Trp and Glu residues for recognition of mRNA cap structure. *FEBS Lett*. 1991; 280, pp. 207–210.

16. Haghighat A, Sonenberg N. eIF4G dramatically enhances the binding of eIF4E to the mRNA 5'-cap structure. *J Biol Chem*.1997 Aug 29; 272(35):21677-80.
17. Willis AE. Translational control of growth factor and proto-oncogene expression. *Int J Biochem Cell Biol*. 1999 Jan; 31(1):73-86.
18. Kozak M. Circumstances and mechanisms of inhibition of translation by secondary structure in eucaryotic mRNAs. *Mol Cell Biol*. 1989 November; 9(11): 5134–5142.
19. Pelletier, J., Sonenberg, N. Photochemical cross-linking of cap binding proteins to eucaryotic mRNAs: Effect of mRNA 5’ secondary structure. *Mol. Cell. Biol*. 1985b; 5:3222–3230.
20. Preiss T, W Hentze M. Starting the protein synthesis machine: eukaryotic translation initiation. *Bioessays*. 2003 Dec; 25(12):1201-11.

21. Marintchev A, Edmonds KA, Marintcheva B, Hendrickson E, Oberer M, Suzuki C, Herdy B, Sonenberg N, Wagner G. Topology and regulation of the human eIF4A/4G/4H helicase complex in translation initiation. *Cell.* 2009 Feb 6; 136(3):447-60.

22. Rogers, G. W., Jr., Komar, A. A., and Merrick, W. C. eIF4A: The godfather of the DEAD box helicases. *Prog. Nucleic Acid Res. Mol. Biol*. 2002; 72, 307–331.

23. Sonenberg N, Dever TE. Eukaryotic translation initiation factors and regulators. Curr Opin Struct Biol. 2003;13(1):56–63

24. Robert F, Pelletier J. Translation initiation: a critical signalling node in cancer. *Expert Opinion Therapeutic Targets*. 2009 Nov; 13(11):1279-93.

25. Marcotrigiano J, Gingras AC, Sonenberg N, Burley SK. *Mol Cell*. 1999; 3: 707–716.

26. Tait S, Dutta K, Cowburn D, Warwicker J, Doig AJ, McCarthy JE. Local control of a disorder-order transition in 4E-BP1 underpins regulation of translation via eIF4E. *Proc Natl Acad Sci U S A*. 2010 Oct 12; 107(41):17627-32.

27. Thumma SC, Kratzke RA. Translational control: a target for cancer therapy. *Cancer Lett*. 2007 Dec 8;258(1):1-8.

28. Gingras AC, Gygi SP, Raught B, Polakiewicz RD, Abraham RT, Hoekstra MF, Aebersold R, Sonenberg N. Regulation of 4E-BP1 phosphorylation: a novel two-step mechanism. *Genes Dev.* 1999; 13:1422–1437

29. Shah OJ, Anthony JC, Kimball SR, Jefferson LS. 4E-BP1 and S6K1: translational integration sites for nutritional and hormonal information in muscle. *Am J Physiol Endocrinol Metab*. 2000 Oct;279(4):E715-29.

30. LoPiccolo J, Blumenthal GM, Bernstein WB, Dennis PA. Targeting the PI3K/Akt/mTOR pathway: effective combinations and clinical considerations. *Drug Resist Updat*. 2008 Feb-Apr; 11(1-2):32-50

31. Hay N, Sonenberg N. Upstream and downstream of mTOR. *Genes Dev*. 2004 Aug 15;18(16):1926-45

32. Holz MK, Ballif BA, Gygi SO, Blenis J. mTOR and S6K1 mediate assembly of the translation preinitiation complex through dynamic protein interchange and ordered phosphorylation events. *Cell*. 2005; 123:569-580

33. Cencic R, Robert F, Pelletier J. Identifying small molecule inhibitors of eukaryotic translation initiation. *Methods Enzymol*. 2007; 431:269-302.

34 Harris TE, Chi A, Shabanowitz J, Hunt DF, Rhoads RE, Lawrence Jr JC. mTOR-dependent stimulation of the association of eIF4G and eIF3 by insulin. *EMBO J*. 2006; 25: 1659–1668.

35 . Lindqvist L, Pelletier J. Inhibitors of translation initiation as cancer therapeutics. *Future Med Chem.* 2009 Dec;1(9):1709-22.

36. Thornton S, Anand N, Purcell D and Lee J. Not just for housekeeping: protein initiation and elongation factors in cell growth and tumorigenesis. *J. Mol. Med.* 2003, 81, 536–548.

37. Schneider RJ, Sonenberg N. Control in Biology and Medicine, Translational control in cancer development, eds Mathews MB, Sonenberg N, Hershey JWB *Cold Spring Harbor Lab Press*. 2007; pp 401–432.

38. Lazaris-Karatzas A, Montine KS Sonenberg N. Malignant transformation by a eukaryotic initiation factor subunit that binds to mRNA 5' cap. *Nature*. 1990; 345:544-7.

39. Ruggero D, Montanaro L, Ma L, Xu W, Londei P, Cordon-Cardo C Pandolfi PP. The translation factor eIF-4E promotes tumor formation and cooperates with c-Myc in lymphomagenesis. *Nat Med*. 2004; 10:484-6

40. Graff JR, Boghaert ER, De Benedetti A, Tudor DM and Zimmer SG. Reduction of translation initiation factor 4E decreases the malignancy of ras-transformed cloned rat embryo fibroblasts. *Int. J. Cancer*. 1995; 60, 255–263.

41. Fingar DC, Richardson CJ, Tee AR, Cheatham L, Tsou C,Blenis J. mTOR Controls Cell Cycle Progression through Its Cell Growth Effectors S6K1 and

4E-BP1/Eukaryotic Translation Initiation Factor 4E. *Mol Cell Biol*. 2004; 24: 200–216.

42. Lynch M, Fitzgerald C, Johnston KA, Wang S, Schmidt EV. Activated eIF4E-binding protein slows G1 progression and blocks transformation by c-myc without inhibiting cell growth. 2004. *J Biol Chem*. 2004; 279: 3327–3339.
43. Avdulov S, Li S, Michalek V, Burrichter D, Peterson M, Perlman DM, Manivel JC, Sonenberg N, Yee D, Bitterman PB, Polunovsky VA. Activation of translation complex eIF4F is essential for the genesis and maintenance of the malignant phenotype in human mammary epithelial cells. *Cancer Cell*. 2004; 5: 553–563.
44. Mills JR, Hippo Y, Robert F, Chen SM, Malina A, Lin CJ, Trojahn U, Wendel HG, Charest A, Bronson RT, Kogan SC, Nadon R, Housman DE, Lowe SW, Pelletier J. mTORC1 promotes survival through translational control of Mcl-1. *Proc Natl Acad Sci U S A*. 2008 Aug 5;105(31):
45. Wendel HG, Silva RL, Malina A, Mills JR, Zhu H, Ueda T, Watanabe-Fukunaga R, Fukunaga R, Teruya-Feldstein J, Pelletier J, Lowe SW. Dissecting eIF4E action in tumorigenesis. *Genes Dev*. 2007 Dec 15;21(24):3232-7.
46. Scheper GC, van Kollenburg B, Hu J, Luo Y, Goss DJ, Proud CG. Phosphorylation of eukaryotic initiation factor 4E markedly reduces its affinity for capped mRNA. *J Biol Chem* 2002*;* 277*:* 3303-*9*.
47. Koromilas AE, Lazaris-Karatzas A, Sonenberg N. mRNAs containing extensive secondary structure in their 5' non-coding region translate efficiently in cells overexpressing initiation factor eIF-4E. *EMBO J.* 1992;11:4153–4158.
48. Wendel HG, De Stanchina E, Fridman JS, Malina A, Ray S, Kogan S, Cordon-Cardo C, Pelletier J, Lowe SW. Survival signalling by Akt and eIF4E in oncogenesis and cancer therapy. *Nature*. 2004;428:332–7
49. Graff JR, Konicek BW, Vincent TM, Lynch RL, Monteith D, Weir SN, Schwier P, Capen A, Goode RL, Dowless MS, Chen Y, Zhang H, Sissons S, Cox K, McNulty AM, Parsons SH, Wang T, Sams L, Geeganage S, Douglass LE, Neubauer BL, Dean NM, Blanchard K, Shou J, Stancato LF, Carter JH,

Marcusson EG. Therapeutic suppression of translation initiation factor eIF4E expression reduces tumor growth without toxicity. *J Clin Invest*. 2007 Sep;117(9):2638-48.

50. Graff JR, Zimmer SG. Translational control and metastatic progression: Enhanced activity of the mRNA cap-binding protein eIF-4E selectively enhances translation of metastasis-related mRNAs. *Clin. Exp. Met*. 2003;20:265–73.
51. Pelletier J, Sonenberg N. Insertion mutagenesis to increase secondary structure within the 5' noncoding region of a eukaryotic mRNA reduces translational efficiency. *Cell*. 1985;40:515–26.
52. Hsieh AC, Ruggero D. Targeting eukaryotic translation initiation factor 4E (eIF4E) in cancer. *Clin Cancer Res*. 2010 Oct 15;16(20):4914-20.
53. Grolleau A., Bowman J., Pradet-Balade B., Puravs E., Hanash S., Garcia-Sanz J.A., Beretta L. Global and specific translational control by rapamycin in T cells uncovered by microarrays and proteomics. *J. Biol. Chem*. 2002; 277:22175–22184
54. Cencic R, Carrier M, Galicia-Vázquez G, Bordeleau ME, Sukarieh R, Bourdeau A, Brem B, Teodoro JG, Greger H, Tremblay ML, Porco JA Jr, Pelletier J. Antitumor activity and mechanism of action of the cyclopenta[b]benzofuran, silvestrol. PLoS One. 2009;4(4):e5223.
55. Graff JR, Zimmer SG. Translational control and metastatic progression: enhanced activity of the mRNA cap-binding protein eIF-4E selectively enhances translation of metastasis-related mRNAs. *Clin Exp Metastasis*. 2003;20(3):265-73.
56. Lin CJ, Cencic R, Mills JR, Robert F, Pelletier J. c-Myc and eIF4F are components of a feedforward loop that links transcription and translation. *Cancer Res*. 2008 Jul 1; 68(13):5326-34.

57. Pérez I, Lin CH, McAfee JG, Patton JG.. Mutation of PTB binding sites causes misregulation of alternative 3' splice site selection in vivo. *RNA*. 1997 Jul; 3(7):764-78.

58. A.D. Ellington, J.W. Szostak. *In vitro* selection of RNA molecules that bind specific ligands. *Nature*. 1990 Aug 30;346(6287):818-22.

59. Mili S, Steitz JA. Evidence for reassociation of RNA-binding proteins after cell lysis: implications for the interpretation of immunoprecipitation analyses. *RNA*. 2004;10:1692–1694.

60. Darnell JC, Fraser CE, Mostovetsky O, Stefani G, Jones TA, Eddy SR, Darnell RB. Kissing complex RNAs mediate interaction between the Fragile-X mental retardation protein KH2 domain and brain polyribosomes. *Genes Dev*. 2005 Apr 15; 19(8):

61. Darnell JC, Mostovetsky O, Darnell RB. FMRP RNA targets: identification and validation. *Genes Brain Behav*. 2005;4:341–349.

62. Schoemaker HJ, Schimmel PR. Photo-induced joining of a transfer RNA with its cognate aminoacyl-transfer RNA synthetase. *J Mol Biol*. 1974; 84:503–513

63. Gilmour DS, Lis JT. Detecting protein-DNA interactions in vivo: distribution of RNA polymerase on specific bacterial genes. *Proc Natl Acad Sci U S A*. 1984; 81:4275–4279.

64. Fecko CJ, Munson KM, Saunders A, Sun G, Begley TP, Lis JT, Webb WW. Comparison of femtosecond laser and continuous wave UV sources for protein-nucleic acid crosslinking. *Photochem Photobiol*. 2007; 83:1394–1404.

65. Urlaub H, Hartmuth K, Luhrmann R. A two-tracked approach to analyze RNA-protein crosslinking sites in native, nonlabeled small nuclear ribonucleoprotein particles. *Methods*. 2002; 26:170–18

66. Brimacombe R, Stiege W, Kyriatsoulis A, Maly P. Intra-RNA and RNA-protein cross-linking techniques in Escherichia coli ribosomes. *Methods Enzymol*. 1988; 164:287–309.

67. Hockensmith JW, Kubasek WL, Vorachek WR, von Hippel PH. Laser cross-linking of nucleic acids to proteins. Methodology and first applications to the phage T4 DNA replication system. *J Biol Chem*. 1986 Mar 15;261(8):3512-8.

68. Kudla G, Granneman S, Hahn D, Beggs JD, Tollervey D. Cross-linking, ligation, and sequencing of hybrids reveals RNA-RNA interactions in yeast. Proc *Natl Acad Sci U S A*. 2011 Jun 14; 108(24):10010-5.

69. Brimacombe R, Stiege W, Kyriatsoulis A, Maly P. Intra-RNA and RNA-protein cross-linking techniques in Escherichia coli ribosomes. *Methods Enzymol*. 1988;164:287–309

70. Dreyfuss G, Choi YD, Adam SA. Characterization of heterogeneous nuclear RNA-protein complexes in vivo with monoclonal antibodies. *Mol Cell Biol*. 1984; 4:1104–1114.

71. Xue Y, Zhou Y, Wu T, Zhu T, Ji X, Kwon YS, Zhang C, Yeo G, Black DL, Sun H, Fu XD, Zhang Y. Genome-wide analysis of PTB-RNA interactions reveals a strategy used by the general splicing repressor to modulate exon inclusion or skipping. *Mol Cell*. 2009;36:996–1006.

72. Yeo GW, Coufal NG, Liang TY, Peng GE, Fu XD, Gage FH. An RNA code for the FOX2 splicing regulator revealed by mapping RNA-protein interactions in stem cells. *Nat Struct Mol Biol*. 2009;16:130–137.

73. Wolf JJ, Dowell RD, Mahony S, Rabani M, Gifford DK, Fink GR. Feed-forward regulation of a cell fate determinant by an RNA-binding protein generates asymmetry in yeast. *Genetics*. 2010 Jun;185(2):513-22

74. Ule J, Jensen KB, Ruggiu M, Mele A, Ule A, Darnell RB. CLIP identifies Nova-regulated RNA networks in the brain. *Science*. 2003;302:1212–1215.

75. Licatalosi DD, Mele A, Fak JJ, Ule J, Kayikci M, Chi SW, Clark TA, Schweitzer AC, Blume JE, Wang X, Darnell JC, Darnell RB. HITS-CLIP yields genome-wide insights into brain alternative RNA processing. *Nature*. 2008;456:464–469.

76. Guil S, Caceres JF. The multifunctional RNA-binding protein hnRNP A1 is required for processing of miR-18a. *Nat Struct Mol Biol*. 2007 ;14:591–596.

77. Van der Brug MP, Blackinton J, Chandran J, Hao LY, Lal A, Mazan-Mamczarz K, Martindale J, Xie C, Ahmad R, Thomas KJ, Beilina A, Gibbs JR, Ding J, Myers AJ, Zhan M, Cai H, Bonini NM, Gorospe M, Cookson MR. RNA binding activity of the recessive parkinsonism protein DJ-1 supports involvement in multiple cellular pathways. *Proc Natl Acad Sci U S A*. 2008; 105:10244–10249.

78. Bohnsack MT, Martin R, Granneman S, Ruprecht M, Schleiff E, Tollervey D. Prp43 bound at different sites on the pre-rRNA performs distinct functions in ribosome synthesis. *Mol Cell*. 2009; 36:583–592.

79. König J, Zarnack K, Rot G, Curk T, Kayikci M, Zupan B, Turner DJ, Luscombe NM, Ule J. iCLIP reveals the function of hnRNP particles in splicing at individual nucleotide resolution. *Nat Struct Mol Biol*. 2010 Jul; 17(7):909-15.

80. Hafner M, Landthaler M, Burger L, Khorshid M, Hausser J, Berninger P, Rothballer A, Ascano M, Jungkamp AC, Munschauer M, Ulrich A, Wardle GS, Dewell S, Zavolan M, Tuschl T. PAR-CliP--a method to identify transcriptome-wide the binding sites of RNA binding proteins. *J Vis Exp*. 2010 Jul 2;(41). pii: 2034.

81. Darnell JC, Van Driesche SJ, Zhang C, Hung KY, Mele A, Fraser CE, Stone EF, Chen C, Fak JJ, Chi SW, Licatalosi DD, Richter JD, Darnell RB. FMRP stalls ribosomal translocation on mRNAs linked to synaptic function and autism. *Cell*. 2011 Jul 22; 146(2):247-61.

82. Konig J, Zarnack K, Rot G, Curk T, Kayikci M, Zupan B, Turner DJ, Luscombe NM, Ule J. iCLIP--transcriptome-wide mapping of protein-RNA interactions with individual nucleotide resolution. *J Vis Exp*. 2011 Apr 30;(50). pii: 2638

83. Libri V, Helwak A, Miesen P, Santhakumar D, Borger JG, Kudla G, Grey F, Tollervey D, Buck AH. Murine cytomegalovirus encodes a miR-27 inhibitor disguised as a target. *Proc Natl Acad Sci U S A*. 2012 Jan 3;109(1):279-84.

84. Granneman S, Kudla G, Petfalski E, Tollervey D. Identification of protein binding sites on U3 snoRNA and pre-rRNA by UV cross-linking and high-throughput analysis of cDNAs. Proc Natl Acad Sci U S A. 2009;106:9613–9618.

85. Robert B. Darnell. HITS-CLIP: panoramic views of protein-RNA regulation in living cells. *Wiley Interdiscip Rev RNA*. 2010 Sep-Oct; 1(2): 266–286.

86. Muñoz MJ, Pérez Santangelo MS, Paronetto MP, de la Mata M, Pelisch F, Boireau S, Glover-Cutter K, Ben-Dov C, Blaustein M, Lozano JJ, Bird G, Bentley D, Bertrand E, Kornblihtt AR. DNA damage regulates alternative splicing through inhibition of RNA polymerase II elongation. *Cell.* 2009;137:708–720.

87. Pelletier, J., Sonenberg, N. Photochemical cross-linking of cap binding proteins to eucaryotic mRNAs: Effect of mRNA 5' secondary structure. *Mol. Cell. Biol*. 1985b; 5:3222–3230.

88.Ho SN, Hunt HD, Horton RM, Pullen JK, Pease LR. Site-directed mutagenesis by overlap extension using the polymerase chain reaction. Gene. 1989 Apr 15;77(1):51-9.

89. Monroy G, Spencer E, Hurwitz J. Characteristics of reactions catalyzed by purified guanylyltransferase from vaccinia virus. *J Biol Chem*. 1978 Jun 25; 253(12):4490-8.

90 Ulmanen, I., B. A. Broni, and R. M. Krug. Role of two of the influenza virus core P proteins in recognizing cap 1 structures (m7GpppNm) on mRNAs and in initiating viral RNA transcription. *Proc. Natl. Acad. Sci. USA*. 1981 78:7355-7359.

91. Cencic R, Desforges M, Hall DR, Kozakov D, Du Y, Min J, Dingledine R, Fu H, Vajda S, Talbot .PJ, Pelletier J. Blocking eIF4E-eIF4G interaction as a strategy to impair coronavirus replication. *J Virol*. 2011 Jul; ;85(13):6381-9.

xcii. Ule J, Jensen K, Mele A, Darnell RB. CLIP: a method for identifying protein-RNA interaction sites in living cells. *Methods*. 2005 Dec; 37(4):376-86.

93. Shola DT, Wang H, Wahdan-Alaswad R, Danielpour D.Hic-5 controls BMP4 responses in prostate cancer cells through interacting with Smads 1, 5 and 8. *Oncogenes*. 2011 Sep 26.

94. Hafner M, Landthaler M, Burger L, Khorshid M, Hausser J, Berninger P, Rothballer A, Ascano M Jr, Jungkamp AC, Munschauer M, Ulrich A, Wardle GS, Dewell S, Zavolan M, Tuschl T. Transcriptome-wide identification of RNA-binding protein and microRNA target sites by PAR-CLIP. Transcriptome-wide identification of RNA-binding protein and microRNA target sites by PAR-CLIP. *Cell*. 2010 Apr 2; 141(1):129-41.

95. Schwartz DC, Parker R. mRNA decapping in yeast requires dissociation of the cap binding protein, eukaryotic translation initiation factor 4E. *Mol Cell Biol*. 2000 Nov;20(21):7933-42.

96. Murata T., Shimotohno K., Shimotohno K. Ubiquitination and proteasome-dependent degradation of human eukaryotic translation initiation factor 4E. *J. Biol. Chem*. 2006;281:20788–20800.

97. Ptushkina M, von der Haar T, Karim MM, Hughes JM, McCarthy JEG. Repressor binding to a dorsal regulatory site traps human eIF4E in a high cap-affinity state. *EMBO J*. 1999;18:4068–4075.

98. Markus Hafner, Markus Landthaler, Lukas Burger, Mohsen Khorshid, Jean Hausser, Philipp Berninger, Andrea Rothballer, Manuel Ascano, Anna-Carina Jungkamp, Mathias Munschauer, Alexander Ulrich, Greg S. Wardle, Scott Dewell, Mihaela Zavolan, and Thomas Tuschl. PAR-CliP - A Method to Identify Transcriptome-wide the Binding Sites of RNA Binding Proteins. *J Vis Exp*. 2010; (41): 2034.

99. Lindqvist L, Imataka H, Pelletier J. Cap-dependent eukaryotic initiation factor-mRNA interactions probed by cross-linking. *RNA*. 2008 May; 14(5):960-9.

100. Wakiyama M, Imataka H, Sonenberg N. Interaction of eIF4G with poly(A)-binding protein stimulates translation and is critical for Xenopus oocyte maturation. *Curr Biol*. 2000 Sep 21; 10(18):1147-50.

101. Marcotrigiano, J., Gingras, A.C., Sonenberg, N., Burley, S.K. Cocrystal structure of the messenger RNA 5' cap-binding protein (eIF4E) bound to 7-methyl-GDP. *Cell* 1997; 89:951–961.

102. Pyronnet S, Imataka H, Gingras AC, Fukunaga R, Hunter T, Sonenberg N. Human eukaryotic translation initiation factor 4G (eIF4G) recruits mnk1 to phosphorylate eIF4E. *EMBO J*. 1999 Jan 4;18(1):270-9.

103. Murata T., Shimotohno K., Shimotohno K. Ubiquitination and proteasome-dependent degradation of human eukaryotic translation initiation factor 4E. *J. Biol. Chem.* 2006;281:20788–20800.

104. Ptushkina M, von der Haar T, Vasilescu S, Frank R, Birkenhäger R, McCarthy JE. Cooperative modulation by eIF4G of eIF4E-binding to the mRNA 5' cap in yeast involves a site partially shared by p20. *EMBO J*. 1998 Aug 17;17(16):4798-808.

105. Khaleghpour K, Pyronnet S, Gingras AC, Sonenberg N. Translational homeostasis: eukaryotic translation initiation factor 4E control of 4E-binding protein 1 and p70 S6 kinase activities. *Mol Cell Biol*. 1999 Jun; 19(6):4302-10.

106. Tesson L, Usal C, Ménoret S, Leung E, Niles BJ, Remy S, Santiago Y, Vincent AI, Meng X, Zhang L, Gregory PD, Anegon I, Cost GJ. Knockout rats generated by embryo microinjection of TALENs. *Nat Biotechnol*. 2011 Aug 5; 29(8):695-6.